Synthesis and Evaluation of Pyrazine and Quinoxaline Fluorophores for in Vivo Detection of Cerebral Tau Tangles in Alzheimer's Models

Biyue Zhu,[a] Ting Zhang,[a] Qian Jiang,[a] Ying Li,[a] Yu Fu,[a] Jiapei Dai,[b] Ge Li,[c] Qingrong Qi,*[, a] Yan Cheng*[, a]

[a]Key Laboratory of Drug-Targeting and Drug Delivery System of the Education Ministry, Sichuan Engineering Laboratory for Plant-Sourced Drug and Sichuan Research Center for Drug Precision Industrial Technology, West China School of Pharmacy, Sichuan University, Chengdu 610041, China

[b]Wuhan Institute for Neuroscience and Neuroengineering, South-Central University for Nationalities, Wuhan 430074, China

[c]Guangdong Laboratory Animals Monitoring Institute, Guangdong Provincial Key Laboratory of Laboratory Animals, Guangzhou 510663, China

*To whom correspondence should be addressed: Phone: +86-28-85501566, Fax: +86-28-85501615. E-mail: yancheng@scu.edu.cn for Y. Cheng. Phone: +86-28-85502157, e-mail: qiqinrong@ scu.edu.cn for Q. Qi.

Keywords: Alzheimer's disease, tau tangles, fluorescence probe, in vivo imaging, tau transgenic mouse

Contents

1. Experimental Section 3

2. ^{1}H-NMR, ^{13}C-NMR, HRMS of QNNs 12

3. Spectroscopic Measurements 24

4. Binding Behavior 27

5. Fluorescence Staining of Human Brain Sections 31

6. Immunocytochemistry of Intracellular Tau Aggregates 32

7. Brain Kinetics in Normal Mice 32

8. Toxicity Studies 34

9. In Vivo Imaging 35

10. References 37

Experimental Section.

General Information. All chemicals were commercial products and used without further purification. ^{1}H-NMR and ^{13}C-NMR spectra were obtained on a VARIAN INOVA 400M NMR spectrometer in $CDCl_3$ solutions with tetramethylsilane (TMS) as an internal standard at room temperature. Chemical shifts are reported as δ values relative to the internal TMS. Coupling constants are reported in Hertz. Multiplicity is defined by s (singlet), d (doublet), t (triplet), and m (multiplet). HRMS was acquired using an Agilent 6410B Triple Quadrupole HPLC/MS system (ESI). HPLC was performed on an Agilent 1260 Infinity Quaternary HPLC system using an Hypersil ODS C_{18} column (250 mm × 4.6 mm, 5 μm) with water/acetonitrile mobile phase delivered at a flow rate of 1.0 mL/min. All synthesized compounds with purities more than 95% determined by analytical HPLC, were used for further evaluation. Kunming mice, nude mice, and C57BL/6 mice were provided by the Laboratory Animal Center of Sichuan University (Chengdu, China). P301S tau transgenic mice were provided by Guangdong Laboratory Animals Monitoring Institute (Guangzhou, China). APP/PS1 transgenic mice were provided by Nanjing Biomedical Research Institute of Nanjing University (Nanjing, China). Animal welfare and experimental protocols were approved by the Sichuan University Animal Ethical Experimentation Committee according to the requirements of the National Act on the use of experimental animals (China).

Synthesis of Pyrazines (1-4 a). To a solution of 2-methylpyrazine (284.5 mg, 3.0 mmol) and *t*-BuOK (448.3 mg, 4.0 mmol) in THF (20 mL) was added the

corresponding aldehyde (2.0 mmol). The mixture was stirred under nitrogen for 2 h at 80 °C. After cooling to room temperature, the solvent was removed and the residue was purified by column chromatography.

Synthesis of Quinoxalines (1-4 b). To a mixture of 2-methylquinoxaline (288.7 mg, 2.0 mmol) and the corresponding aldehyde (1.0 mmol) in aqueous sodium hydroxide (5.0 M, 15 mL), Aliquat 336 (43.2 mg, 0.1 mmol) was added dropwise. The solution was heated at 110 °C for 15 h and then filtered after cooling to room temperature. The residue was purified by column chromatography.

*(E)-N,N-dimethyl-4-(2-(pyrazin-2-yl)vinyl)aniline (**1a**).* Yellow solid, 208.2 mg, 46.2% yield, 97.7% purity. Mp 124-125 °C. ^{1}H NMR (400 MHz, $CDCl_3$) δ: 8.59 (s, 1H), 8.48 (s, 1H), 8.32 (s, 1H), 7.67 (d, J = 16.0 Hz, 1H), 7.50 (d, J = 8.8 Hz, 2H), 6.95 (d, J = 16.0 Hz, 1H), 6.72 (d, J = 8.4 Hz, 2H), 3.02 (s, 6H). ^{13}C NMR (100 MHz, $CDCl_3$) δ: 152.2, 150.9, 144.1, 143.3, 141.5, 135.4, 128.6, 124.1, 119.2, 112.0, 40.2. HRMS (ESI) Calcd. for $C_{14}H_{15}N_3$ $[M+H]^+$: 226.1344; Found: 226.1353.

*(E)-N,N-dimethyl-4-(2-(quinoxalin-2-yl)vinyl)aniline (**1b**).* Yellow solid, 102.8 mg, 37.3% yield, 98.7% purity. Mp 162-163 °C. ^{1}H NMR (400 MHz, $CDCl_3$) δ: 9.01 (s, 1H), 8.03 (t, J =7.0 Hz, 2H), 7.81 (d, J = 16.4 Hz, 1H), 7.74-7.70 (m, 1H), 7.67-7.63 (m, 1H), 7.57 (d, J = 9.2 Hz, 2H), 7.18 (d, J = 16.0 Hz, 1H), 6.74 (d, J = 8.8 Hz, 2H), 3.04 (s, 6H). ^{13}C NMR (100 MHz, $CDCl_3$) δ: 151.6, 151.1, 144.5, 142.5, 141.1, 136.8, 130.1, 129.0, 128.9, 128.8, 128.5, 124.0, 120.5, 112.1, 40.2. HRMS (ESI) Calcd. for $C_{18}H_{17}N_3$ $[M+H]^+$: 276.1500; Found: 276.1500.

*(E)-N,N-dimethyl-5-(2-(pyrazin-2-yl)vinyl)pyridin-2-amine (**2a**).* Yellow solid,

98.6 mg, 21.8% yield, 99.9% purity. Mp 133-134 °C. ^{1}H NMR (400 MHz, $CDCl_3$) δ: 8.58 (s, 1H), 8.50 (s, 1H), 8.34 (dd, J =5.2 Hz, 2.0 Hz, 2H), 7.77 (dd, J = 8.8 Hz, 2.0 Hz, 1H), 7.65 (d, J = 16.0 Hz, 1H), 6.93 (d, J = 16.0 Hz, 1H), 6.56 (d, J = 8.8 Hz, 1H), 3.15 (s, 6H). ^{13}C NMR (100 MHz, $CDCl_3$) δ: 159.1, 151.8, 148.9, 144.2, 143.4, 141.9, 134.3, 132.4, 119.9, 119.8, 105.9, 38.1. HRMS (ESI) Calcd. for $C_{13}H_{14}N_4$ $[M+H]^+$: 227.1296; Found: 227.1290.

*(E)-N,N-dimethyl-5-(2-(quinoxalin-2-yl)vinyl)pyridin-2-amine (**2b**).* Yellow solid, 105.3 mg, 38.1% yield, 99.8% purity. Mp 186-187 °C. ^{1}H NMR (400 MHz, $CDCl_3$) δ: 8.99 (s, 1H), 8.39 (d, J = 2.0 Hz, 1H), 8.04 (t, J = 7.0 Hz, 1H), 7.83 (dd, J = 9.2 Hz, 2.4 Hz, 1H), 7.78 (d, J = 16.4 Hz, 1H), 7.70 (dd, J = 12.0 Hz, 1.6 Hz, 2H), 7.67 (t, J = 6.8 Hz, 1H), 7.15 (d, J = 16.4 Hz, 1H), 6.59 (d, J = 8.8 Hz, 1H), 3.17 (s, 6H). ^{13}C NMR (100 MHz, $CDCl_3$) δ: 159.2, 151.1, 149.3, 144.5, 142.5, 141.2, 134.4, 133.8, 130.2, 129.1, 128.9, 128.7, 121.0, 119.9, 106.0, 38.1. HRMS (ESI) Calcd. for $C_{17}H_{16}N_4$ $[M+H]^+$: 277.1453; Found: 277.1458.

*(E)-N,N-dimethyl-5-(2-(pyrazin-2-yl)vinyl)thiophen-2-amine (**3a**).* Orange solid, 92.4 mg, 20.0% yield, 99.8% purity. Mp 83-84 °C. ^{1}H NMR (400 MHz, $CDCl_3$) δ: 8.44 (d, J = 13.2 Hz, 2H), 8.24 (d, J = 2.0 Hz, 1H), 7.74 (d, J = 15.2 Hz, 1H), 6.93 (d, J = 4.0 Hz, 1H), 6.49 (d, J = 15.6 Hz, 1H), 5.78 (d, J = 4.0 Hz, 1H), 3.01 (s, 6H). ^{13}C NMR (100 MHz, $CDCl_3$) δ : 160.3, 152.1, 144.1, 143.1, 140.9, 131.5, 129.2, 125.9, 116.5, 102.1, 42.3. HRMS (ESI) Calcd. for $C_{12}H_{13}N_3S$ $[M+Na]^+$:254.0728; Found:254.0727.

*(E)-N,N-dimethyl-5-(2-(quinoxalin-2-yl)vinyl)thiophen-2-amine (**3b**).* Black solid,

98.3 mg, 34.9% yield, 99.4% purity. Mp 142-143 °C. ^{1}H NMR (400 MHz, $CDCl_3$) δ: 8.85 (s, 1H), 7.98 (t, J = 9.2 Hz, 2H), 7.89 (d, J = 15.6 Hz, 1H), 7.71-7.67 (m, 1H), 7.62-7.59 (m, 1H), 7.02 (d, J = 4.0 Hz, 1H), 6.70 (d, J = 15.6 Hz, 1H), 5.81 (d, J = 4.0 Hz, 1H), 3.03 (s, 6H). ^{13}C NMR (100 MHz, $CDCl_3$) δ: 161.0, 151.4, 144.8, 142.6, 140.8, 132.4, 130.6, 130.0, 129.0, 128.5, 128.0, 125.9, 117.4, 102.4, 42.2. HRMS (ESI) Calcd. for $C_{16}H_{15}N_3S$ $[M+H]^+$: 282.1065; Found: 282.1068.

N, N-dimethyl-4-((1E,3E)-4-(pyrazin-2-yl)buta-1,3-dienyl)benzenamine ***(4a)****.* Orange solid, 121.3 mg, 24.1% yield, 96.7% purity. Mp 135-136 °C. ^{1}H NMR (400 MHz, $CDCl_3$) δ: 8.53 (s, 1H), 8.47 (s, 1H), 8.31 (s, 1H), 7.53 (dd, J = 10.0, 15.2 Hz, 1H), 7.39 (s, 1H), 7.37 (s, 1H), 6.86 (d, J = 15.2 Hz, 1H), 6.78 (d, J = 15.2 Hz, 1H), 6.71-6.69 (m, 2H), 6.60 (d, J = 15.2 Hz, 1H), 3.00 (s, 6H). ^{13}C NMR (100 MHz, $CDCl_3$) δ: 152.0, 150.5, 144.2, 143.4, 141.7, 137.5, 136.5, 128.1, 125.1, 124.9, 123.8, 112.2, 40.3. HRMS (ESI): Calcd. for $C_{16}H_{18}N_3$ $[M+H]^+$: 252.1501; Found: 252.1503.

N,N-dimethyl-4-((1E,3E)-4-(quinoxalin-2-yl)buta-1,3-dien-1-yl)aniline ***(4b)****.* Red solid, 89.4 mg, 29.7% yield, 96.9% purity. Mp 127-129 °C. ^{1}H NMR (400 MHz, $CDCl_3$) δ: 8.92 (s, 1H), 8.02 (t, J = 7.2 Hz, 2H), 7.71 (dd, J = 8.0 Hz, 11.2 Hz, 1H), 7.67 (dd, J = 14.2 Hz, 7.2 Hz, 2H), 7.41 (d, J = 8.8 Hz, 2H), 6.89 (d, J = 8.0 Hz, 2H), 6.81 (d, J = 16.0 Hz, 1H), 6.70 (d, J = 8.4 Hz, 2H), 3.01 (s, 6H). ^{13}C NMR (100 MHz, $CDCl_3$) δ: 151.3, 150.6, 144.6, 142.6, 141.1, 138.4, 137.9, 130.1, 129.0, 128.9, 128.7, 128.3, 126.3, 124.8, 123.8, 112.2, 40.3. HRMS (ESI) Calcd. for $C_{20}H_{19}N_3$ $[M+H]^+$: 302.1657; Found: 302.1630.

Preparation of in vitro Tau, Aβ$_{1-42}$ and α-Synuclein Aggregates. Four-repeat

recombinant human tau construct K18 fragment purified from *Escherichia coli* was purchased from ChinaPeptide (China). Tau aggregates were prepared by incubating tau-K18 (55 μM, final concentration) with heparin (110 μM, final concentration) in PBS (0.01 M, pH = 7.4) at 37°C for 3 days with agitation at 100 rpm.[1] Synthetic $A\beta_{1-42}$ peptide (Amresco, USA) was aggregated at a concentration of 55 μM with 1 mM EDTA in PBS (0.01 M, pH = 7.4) at 37 °C for 42 h with agitation at 100 rpm.[2] Recombinant human α-synuclein purified from *Escherichia coli* was purchased from Sino Biological (China). α-synuclein (55 μM, final concentration) was aggregated in PBS (0.01 M, pH = 7.4) at 37 °C for 7 days with agitation at 100 rpm.[3]

Preparation of in vitro Soluble Tau and Aβ Species. Oligomeric and monomeric tau or Aβ were prepared by following previously reported procedures.[4]

Spectral Study. UV/vis and fluorescence spectra were measured by a UV-1800PC spectrophotometer (MAPADA, China) and RF5301PC spectrophotometer (Shimadzu, Japan), respectively. Maximum absorbance wavelength (λ_{abs}), molar absorption coefficient (ε), maximum excitation wavelength (λ_{ex}), maximum emission wavelength (λ_{em}), and fluorescence quantum yield (Φ) were measured in ethanol. To a PBS solution of the probe (1 μM, final concentration) was added 100 μL suspension of tau aggregates, $A\beta_{1-42}$ aggregates or BSA (2.75 μM, final concentration). The mixture was incubated at room temperature for 1 h, and fluorescence spectra were obtained by a fluorescence spectrophotometer. Fluorescence quantum yields (Φ) were calculated by taking Rhodamine B (Sigma, USA; Φ = 0.7 in ethanol) as a reference fluorophore.[5]

In Vitro Saturation Assays. 100 μL of tau aggregates or $A\beta_{1-42}$ aggregates (1.0 μM, final concentration) was added into 400 μL of probe in PBS solution (1, 5, 10, 20, 50, 100, 250, 500, 800 and 1000 nM, final concentration). The mixture was incubated at room temperature for 1 h, transferred to 96-well black plate, and measured using a multifunction microplate reader (Thermo Scientific Varioskan Flash, USA). Dissociation constants (K_d) were calculated using GraphPad Prism 5.0 with nonlinear one-site binding regression (GraphPad Software, USA).

Fluorescence Staining using Human AD Brain Sections. Brain sections from an AD patient were obtained from China brain bank center (6-μm-thick, temporal lobe, male, 85 years old) and were deparaffinized in xylene, 100% ethanol, 95% ethanol, and H_2O. Brain sections were incubated with 1 μM of the probe for 30 min at room temperature, and were then rinsed with 40% ethanol (2 × 1 min) and H_2O (2 × 30 s). Fluorescence images of the sections were obtained under an LSM 800 laser scanning confocal microscope (Zeiss, Germany). The presence of tau tangles was confirmed by subsequent immunostaining of the same section with Alexa Fluor 647-labeled phospho-tau monoclonal antibody AT8 (Thermo Scientific, USA). Imaged brain sections were further incubated with formic acid for 15 min to solubilize filamentous tau, re-stained with probe solution, and observed under the same condition.

Detection of OA-treated Tau Aggregates in SH-SY5Y Cells. Human neuroblastoma cells (SH-SY5Y) were purchased from ATCC (American Type Culture Collection, USA). The cells were seeded at 5×10^5 in a glass-bottom cell culture dish (Nest Biotechnology, China) and cultured in Dulbecco's Modified Eagle's

Medium/F-12 medium with high glucose (Hyclone, USA) supplemented with 10% fetal bovine serum (Gibco, USA), 100 IU/mL penicillin, and 100 μg/mL streptomycin at 37 °C in an atmosphere containing 5% CO_2. Okadaic acid (OA) (100 nM, final concentration) was added into the medium of SH-SY5Y cells for 3 h to induce tau hyperphosphorylation, and intracellular tau aggregates were confirmed by immunocytochemistry. The cells were then treated with probe (2 μM, 1% DMSO/DMEM) for 30 min, washed with PBS for 3 times, fixed in 4% paraformaldehyde, and were observed under an LSM 800 laser scanning confocal microscope. The presence of tau aggregates was confirmed by immunostaining with Alexa Fluor 647 labeled AT8 antibody. After imaging, the cells were further treated with formic acid for 15 min, re-stained with probe solution, and observed under the same condition.

Brain Kinetics in Normal Mice. Kunming mice (n = 3 per timepoint) were intravenously injected with the probe (3.0 mg/kg, 45% DMSO and 55% propylene glycol), and were sacrificed at 2, 10, 30, and 60 min postinjection. Whole brains and blood samples were prepared in acetonitrile and centrifuged at 10000 r for 5 min at 4°C. The leftovers were extracted with acetonitrile for twice and supernatants were collected and analyzed by HPLC. The uptake data was represented by % injected dose per gram (%ID/g).[6]

Cytotoxicity Study. SH-SY5Y cells were seeded into a 96-well plate for 24 h. The cells were then treated with probe solution (0 - 10 μM, 1% DMSO/DMEM). After 24 h incubation, [3-(4,5-dimethylthiazol-2-yl)-2,5-diphenyltetrazolium bromide]

(MTT) solution (5 mg/mL, 20 μL) was added into each well and the cells were further incubated for 4 h. The medium was carefully removed and the formazan crystals were dissolved by 150 μL of DMSO. The absorbance of each well was measured by a multifunction microplate reader at 570 nm. Cells without probe treatment were used as 100% viability. The relative viability (%) was calculated as the absorbance ratio of test sample to that of control.

H&E Histopathology Evaluation. Kunming mice (n = 3 per timepoint) were intravenously injected with probe solution (3.0 mg/kg, 45% DMSO and 55% propylene glycol), and were sacrificed at 1, 3 and 7 days postinjection. Mice with blank solvent injection were used as controls. Whole brains were cut into 6-μm-thick slices using a CM 1950 cryostat (Leica, Germany) and stained with hematoxylin and eosin (H&E). The sections were observed under an Aviovert 40 CFL microscope (Zeiss, Germany) for histopathology evaluation.

In Vivo Imaging. Normal nude mice (n = 3, female, 6 weeks) were used. P301S tau transgenic mice (n = 3, 9-month-old, female), APP/PS1 transgenic mice (n = 3, 9-month-old, female) and C57BL/6 mice (n = 3, 9-month-old, female) were head-shaved before imaging. Mice were anesthetized and intravenously injected with **3b** (3.0 mg/kg, 45% DMSO, 55% propylene glycol). Real-time images were recorded using an IVIS Lumina Series III imaging system (excitation = 500 nm; emission = 620 nm; exposure time = 1 s; gamma = 1.5; brightness = 100; binning = 4; fstop = 2). Regions of interest (ROIs) were drawn around the brain area, and fluorescence intensities of ROIs at each timepoint [*F(t)*] were analyzed by LivingImage Software.

Relative fluorescence intensity (%) at each timepoint was calculated by the following equation:

$$\text{Relative fluorescence intensity (\%)} = [F(t) - F(pre)] / [F(t') - F(pre)] \times 100\%.$$

where $F(pre)$ represents background signals before probe injection; $F(t')$ represents fluorescence signal at timepoint of initial imaging.

Ex Vivo Fluorescence Observation. Mice were sacrificed after in vivo imaging, and whole brains were cut into 6-μm-thick slices using a CM 1950 cryostat (Leica, Germany). Fluorescence observation was performed using an Aviovert 40 CFL fluorescence microscope (Zeiss, Germany) equipped with FITC and Rhodamine B filter sets. The presence of tau tangles or Aβ plaques was confirmed by subsequent staining of the same section with 0.125% ThS.

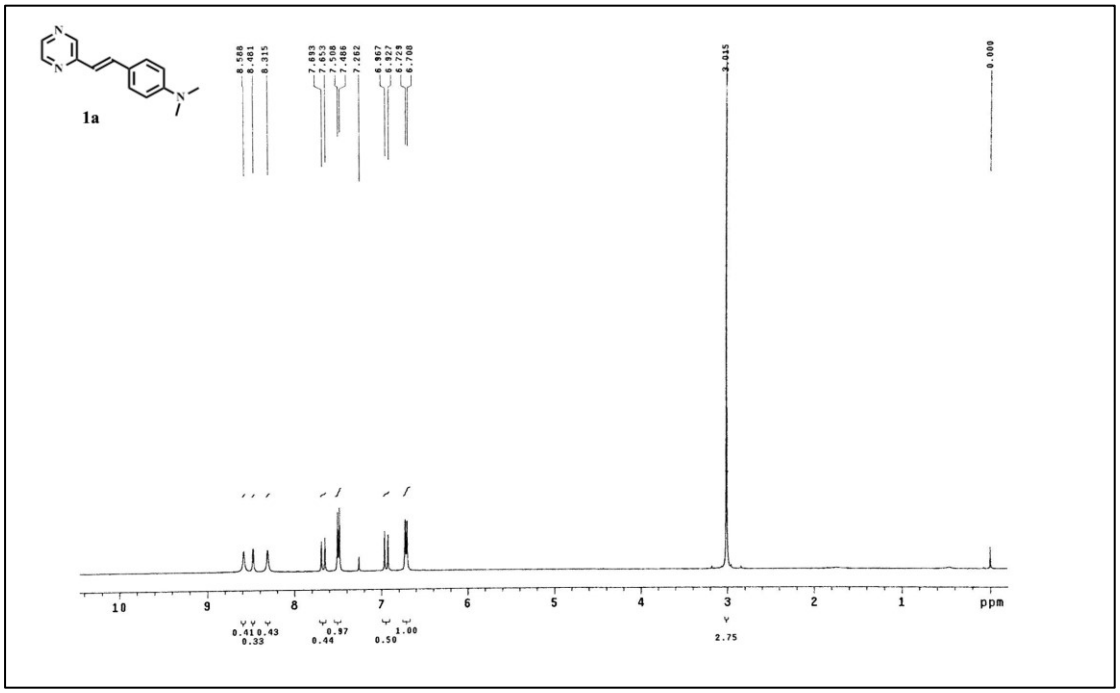
1a
8.568
8.561
8.315
7.693
7.653
7.508
7.486
7.262
6.967
6.927
6.729
6.700
3.015
0.000
10
9
8
7
6
5
4
3
2
1
ppm
0.41
0.43
0.33
0.97
0.44
1.00
0.50
2.75

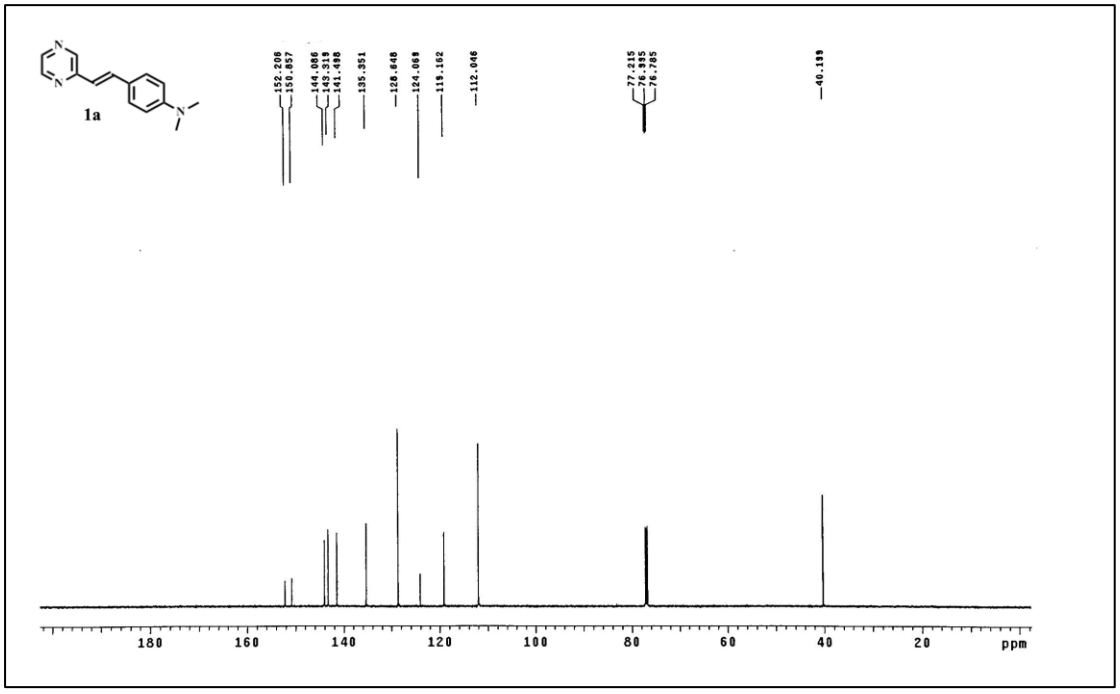
1a
152.208
150.857
144.086
143.319
141.498
135.351
128.648
124.068
119.162
112.046
77.215
76.345
76.785
40.199
180
160
140
120
100
80
60
40
20
ppm

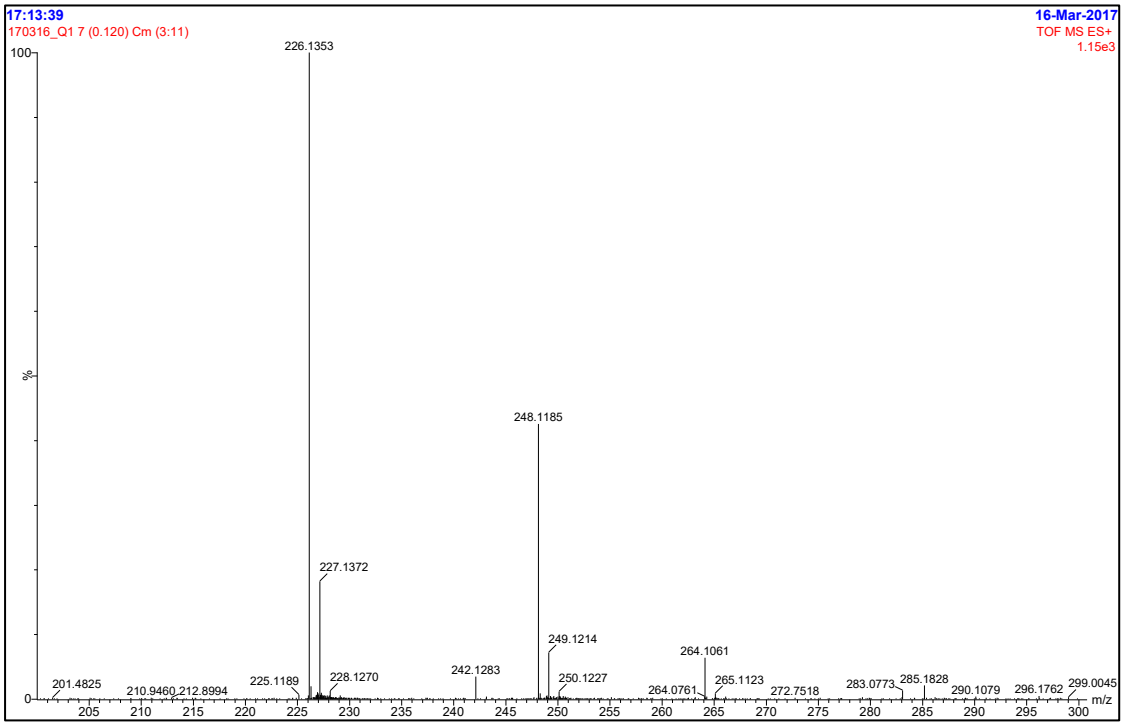

Fig. S1 ^{1}H-NMR, ^{13}C-NMR and HRMS data of **1a**.

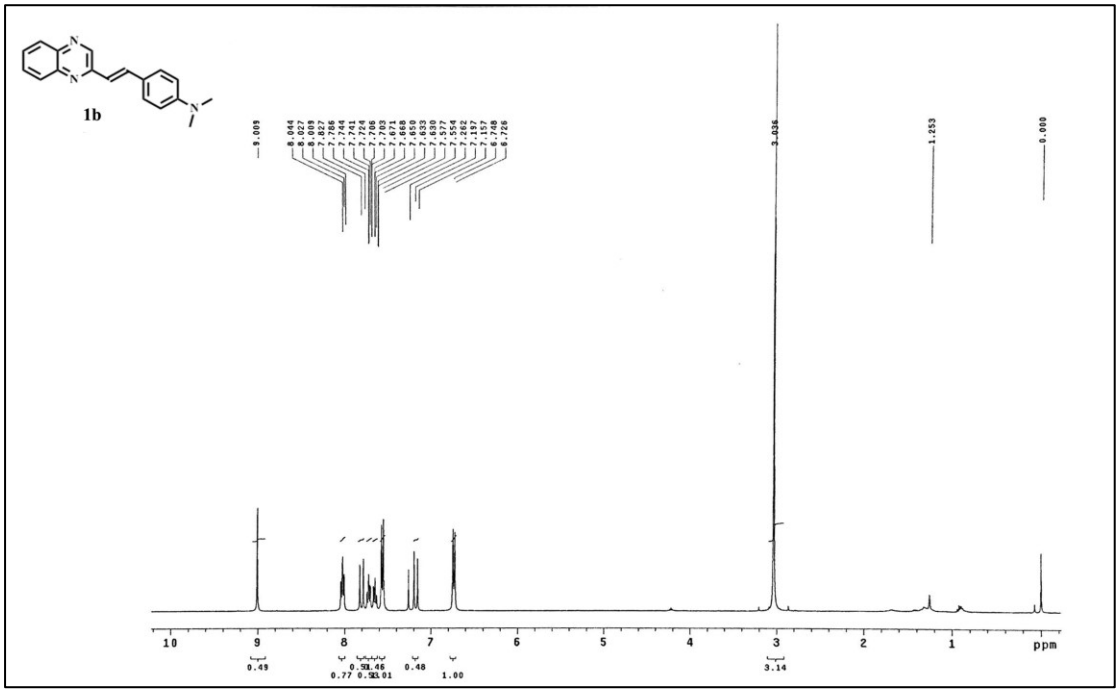

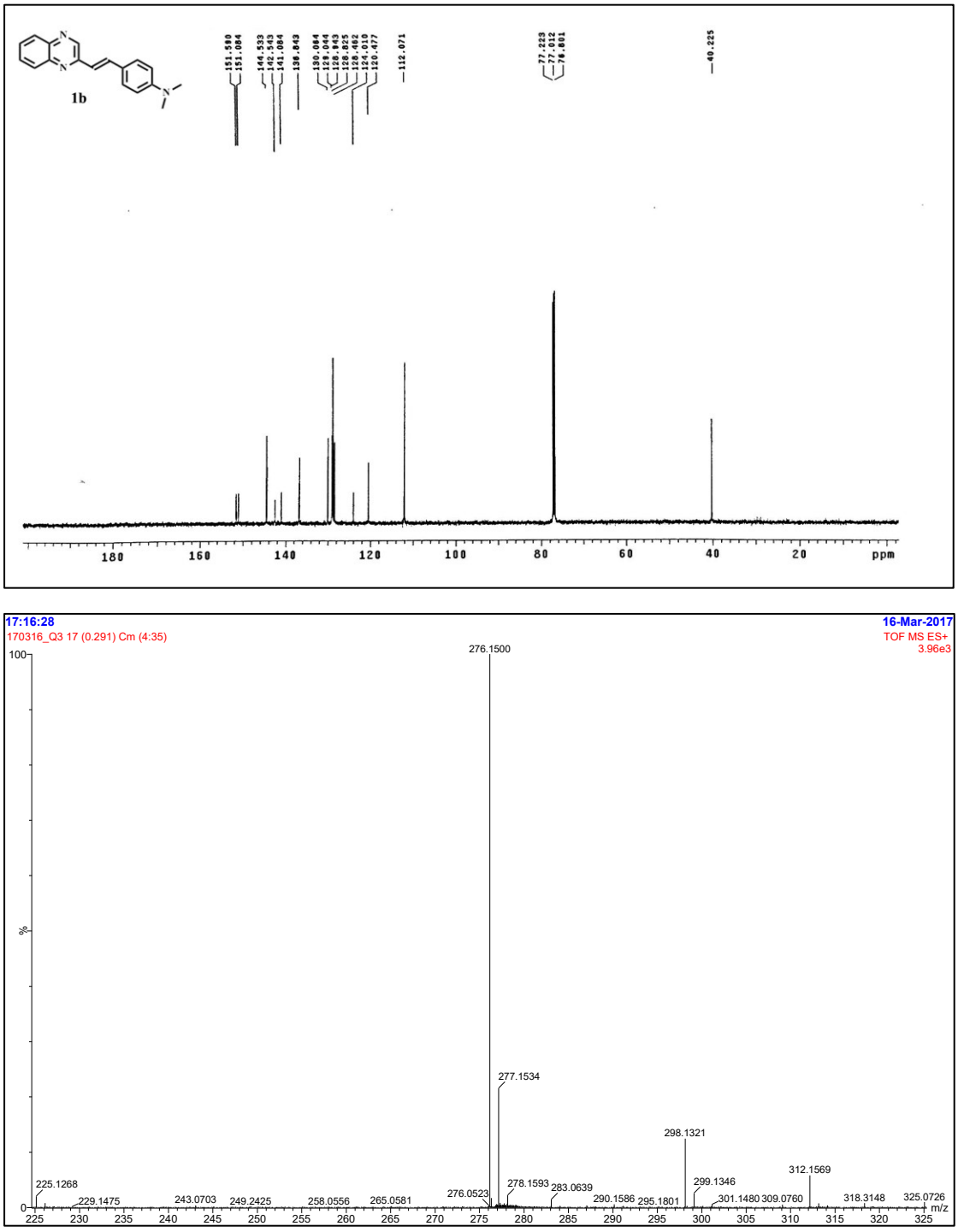

Fig. S2 ^{1}H-NMR, ^{13}C-NMR and HRMS data of **1b**.

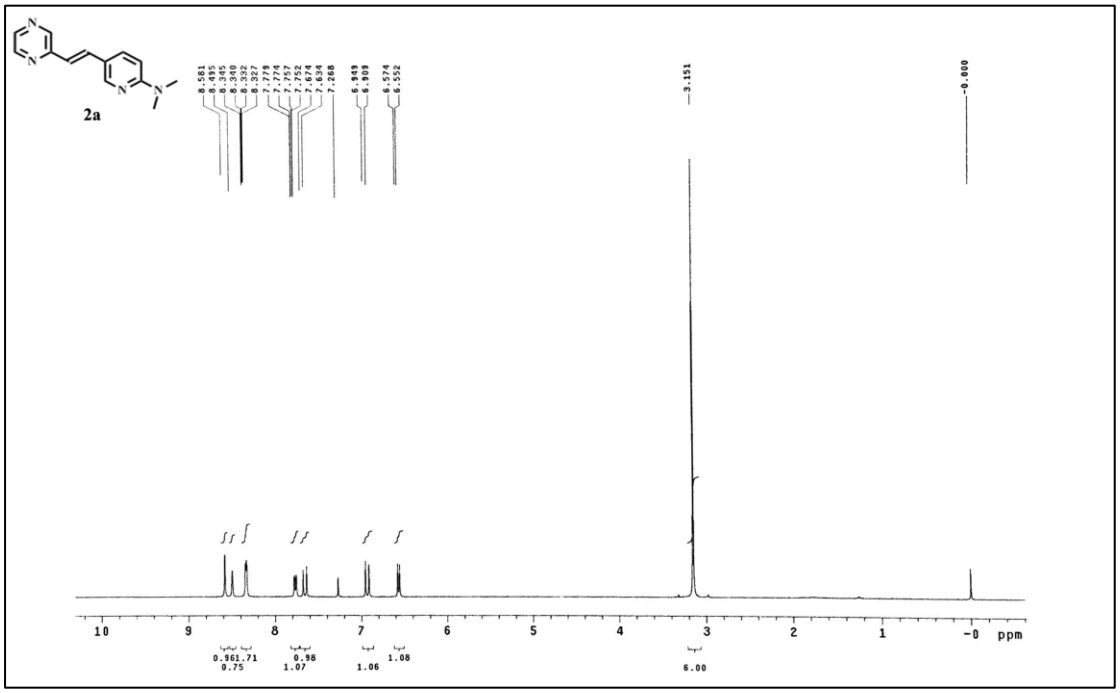
2a
8.581
8.495
8.485
8.340
8.332
8.327
7.778
7.774
7.757
7.752
7.734
7.634
7.266
6.949
6.909
6.574
6.552
3.151
0.000
10
9
8
7
6
5
4
3
2
1
0
ppm
0.961.71
0.75
0.98
1.07
1.06
1.08
6.00

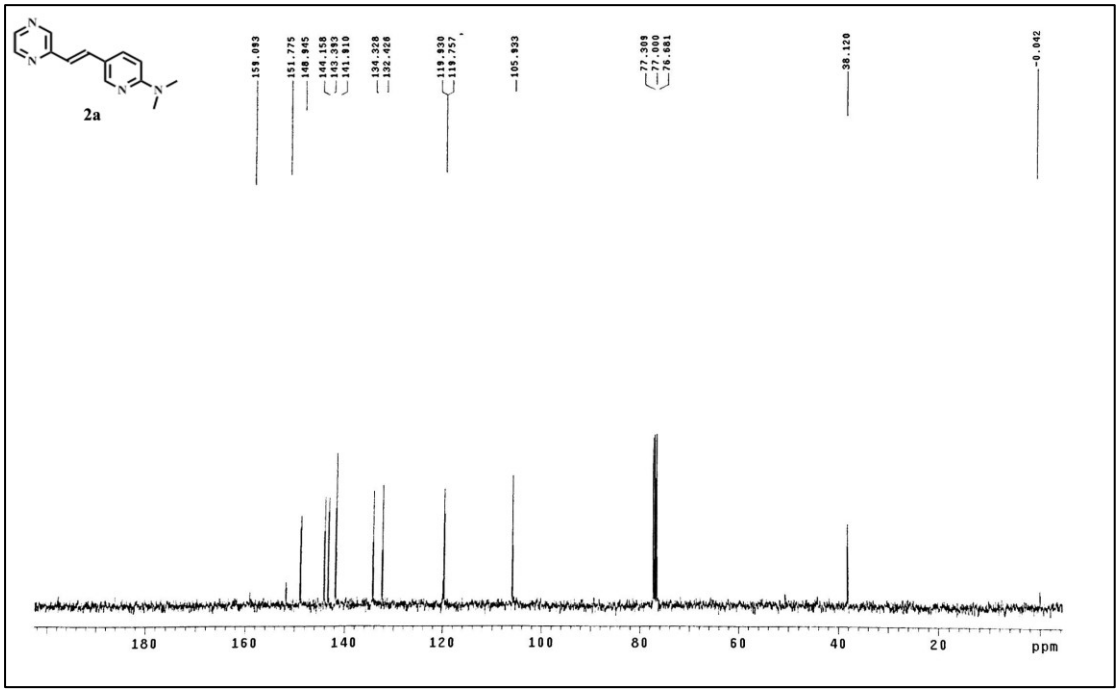
2a
159.093
151.775
148.945
146.158
143.355
141.810
134.328
132.426
119.930
119.757
105.933
77.308
77.000
76.681
38.120
0.042
180
160
140
120
100
80
60
40
20
ppm

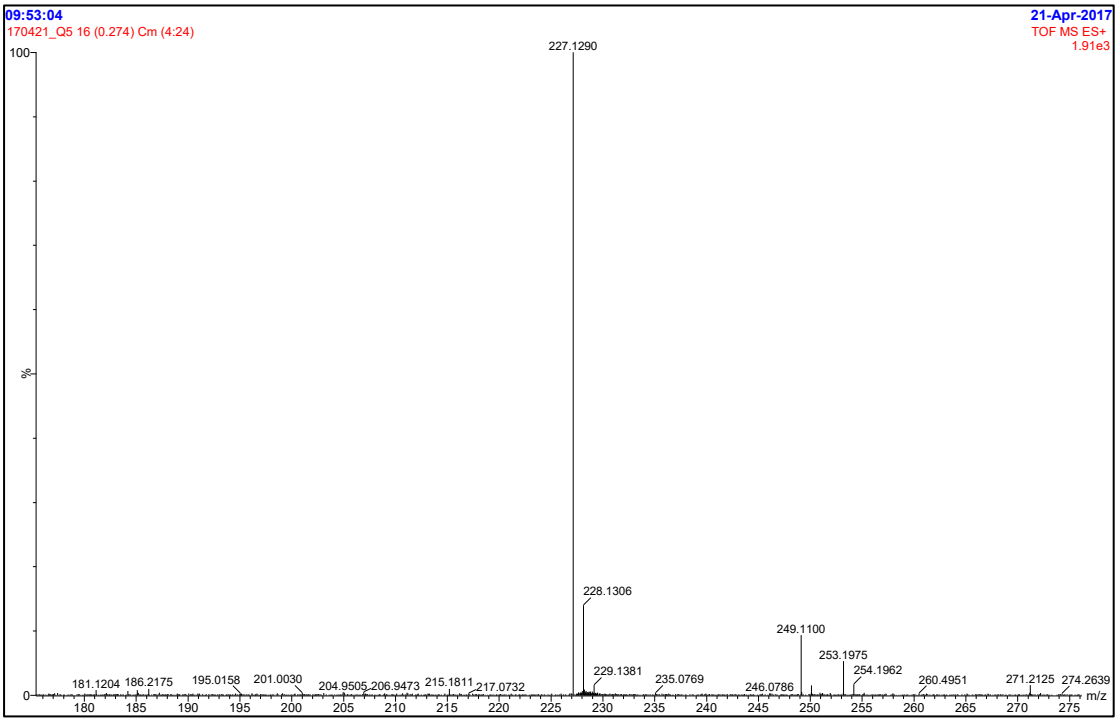

Fig. S3 ^{1}H-NMR, ^{13}C-NMR and HRMS data of **2a**.

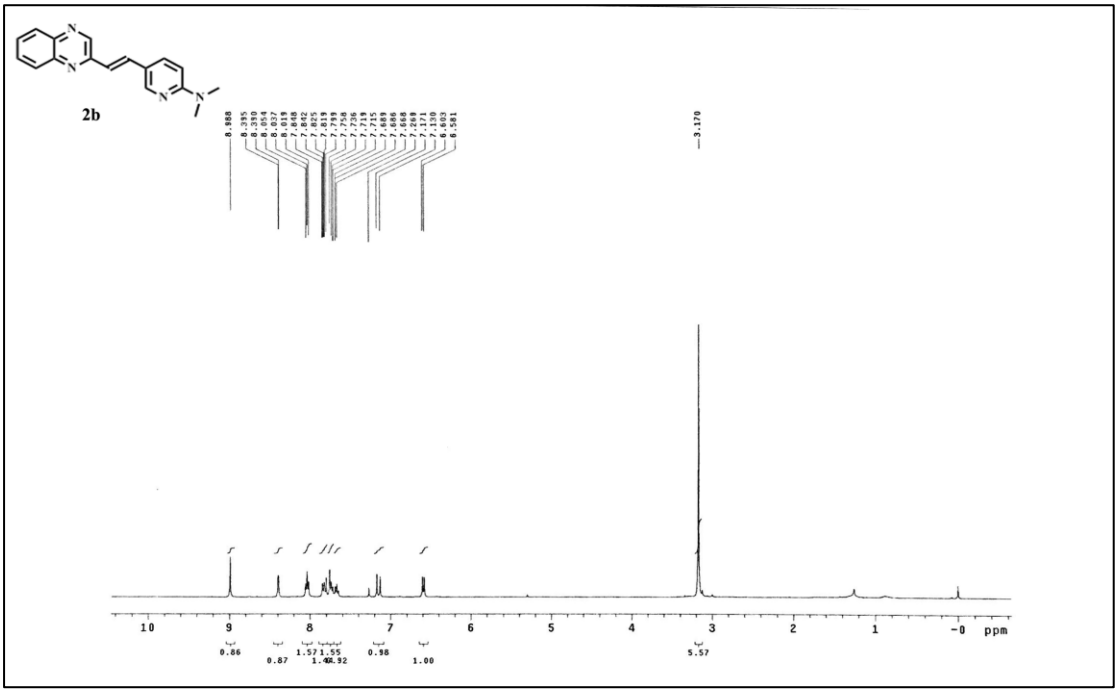

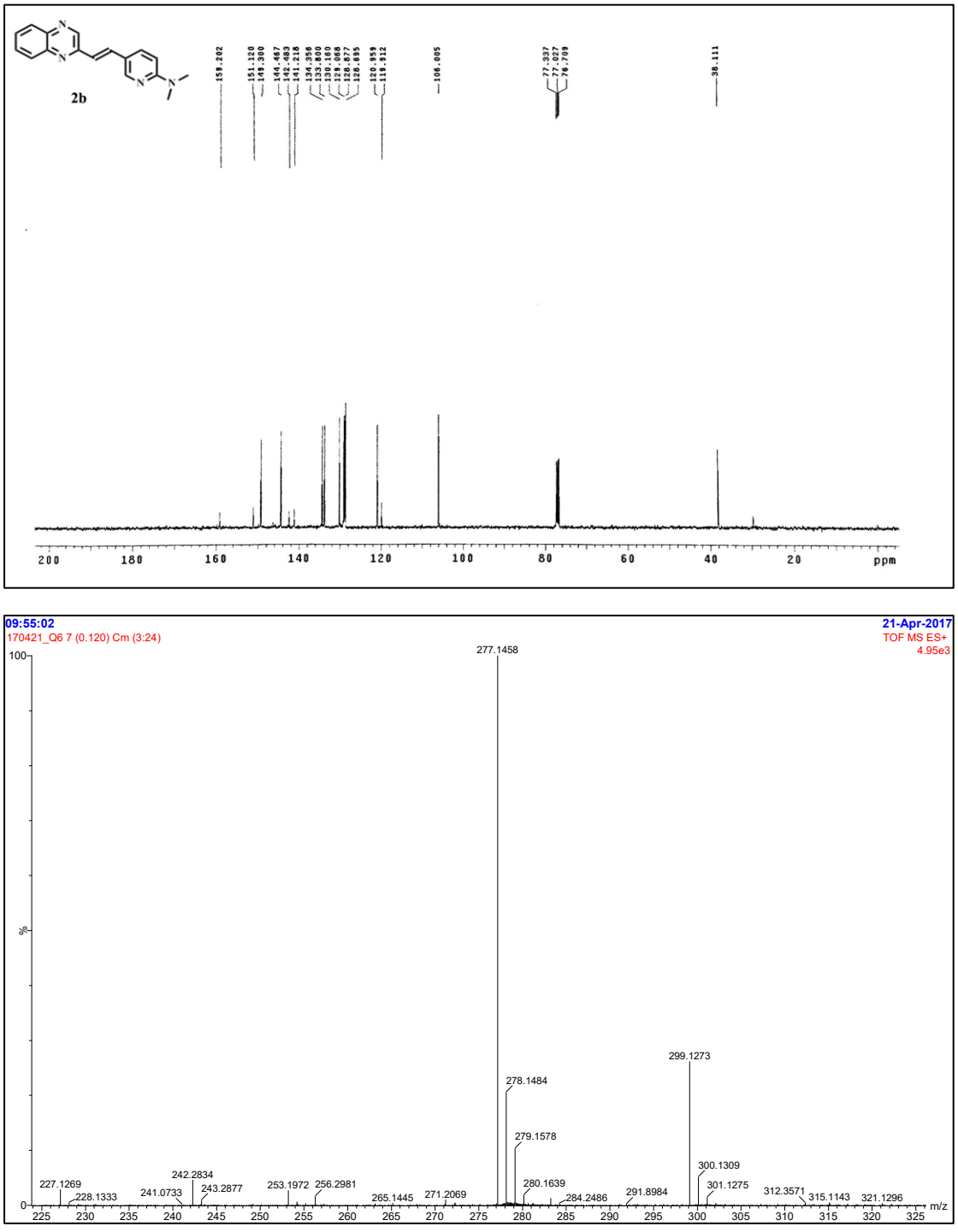

Fig. S4 ^{1}H-NMR, ^{13}C-NMR and HRMS data of **2b**.

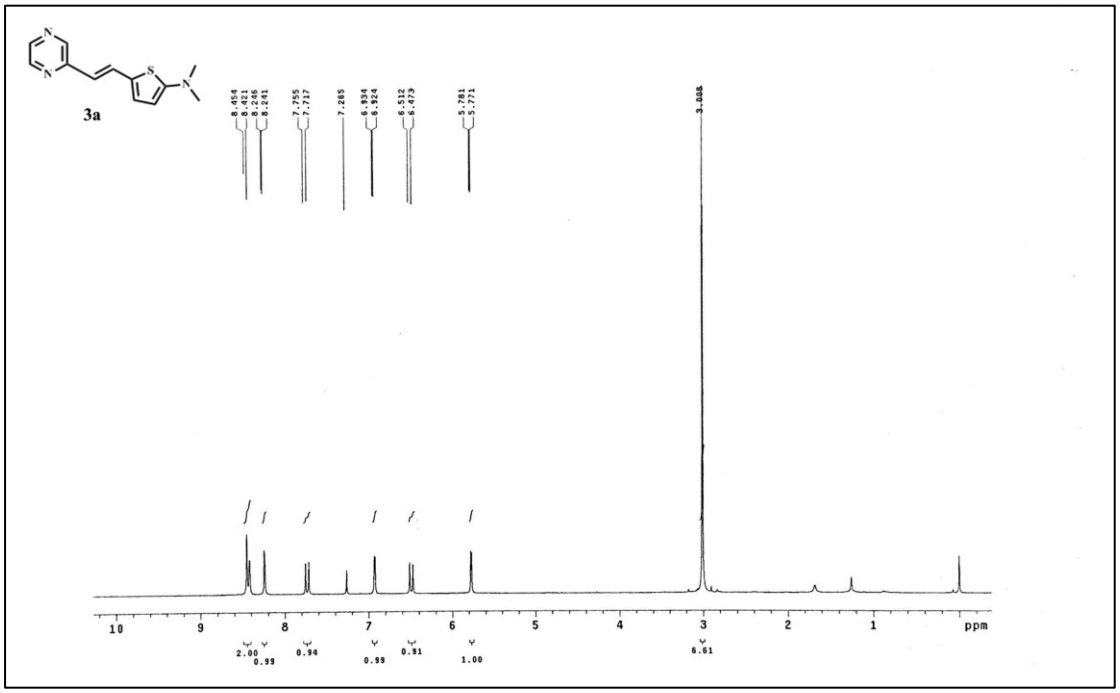
3a
8.454
8.421
8.246
8.141
7.755
7.737
7.265
6.534
6.524
6.512
6.479
5.781
5.771
3.008
10
9
8
7
6
5
4
3
2
1
ppm
2.00
0.99
0.94
0.99
0.91
1.00
6.61

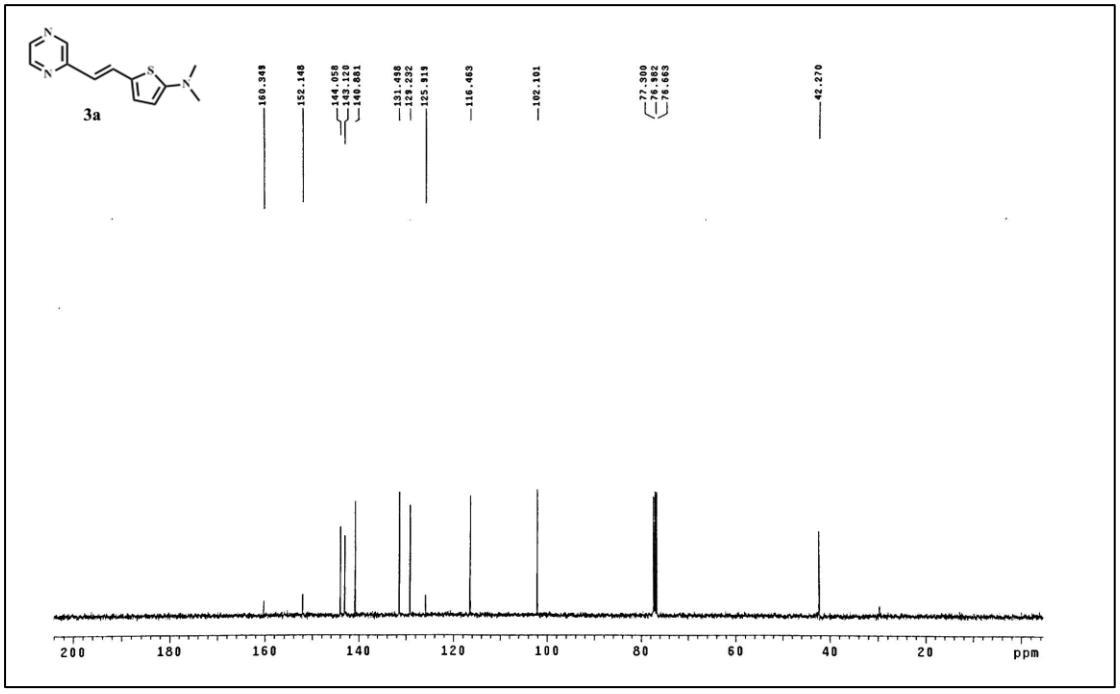
3a
160.349
152.148
144.058
143.120
140.881
131.498
129.232
125.913
116.463
102.101
77.300
76.982
76.663
42.270
200
180
160
140
120
100
80
60
40
20
ppm

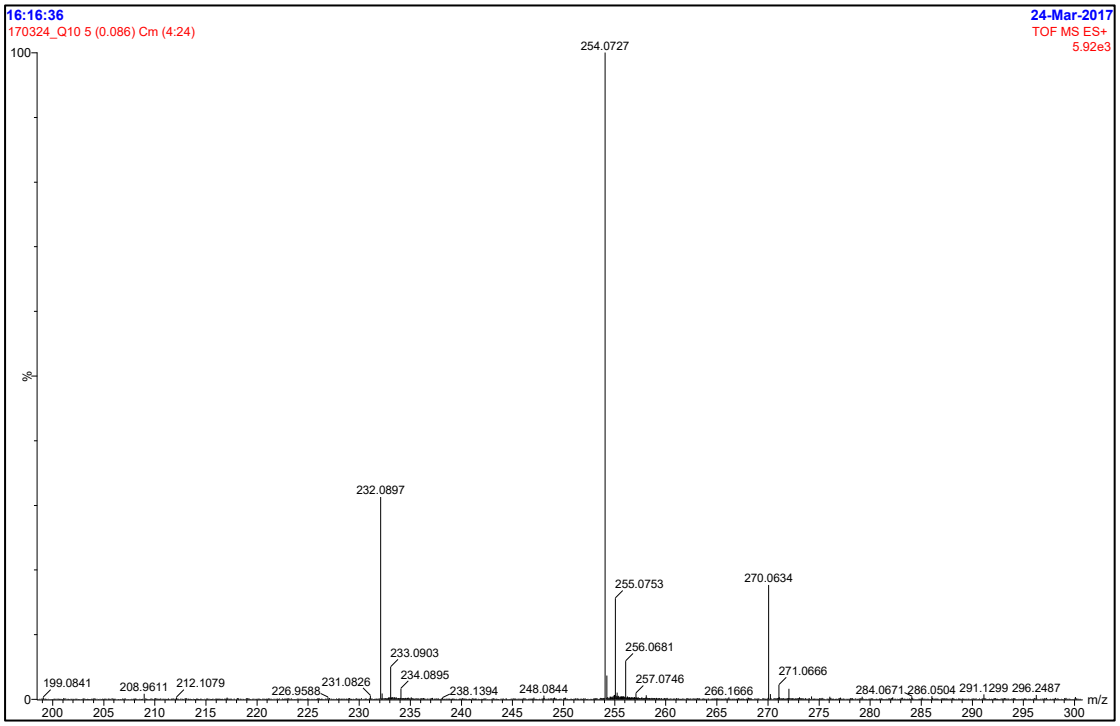

Fig. S5 ^{1}H-NMR, ^{13}C-NMR and HRMS data of **3a**.

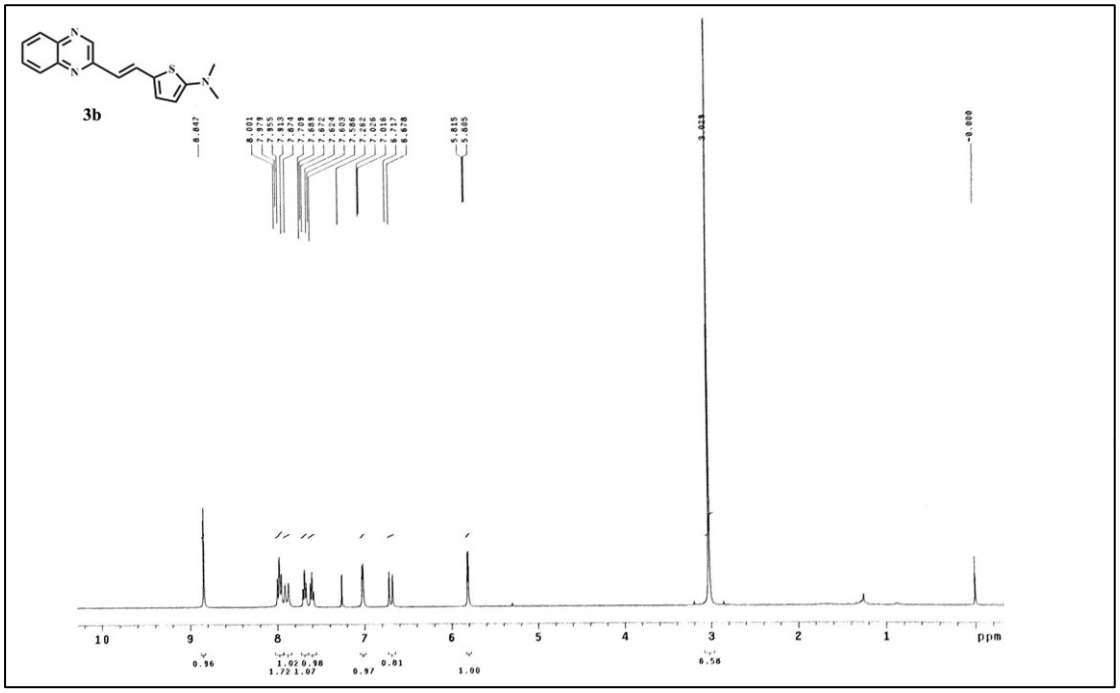

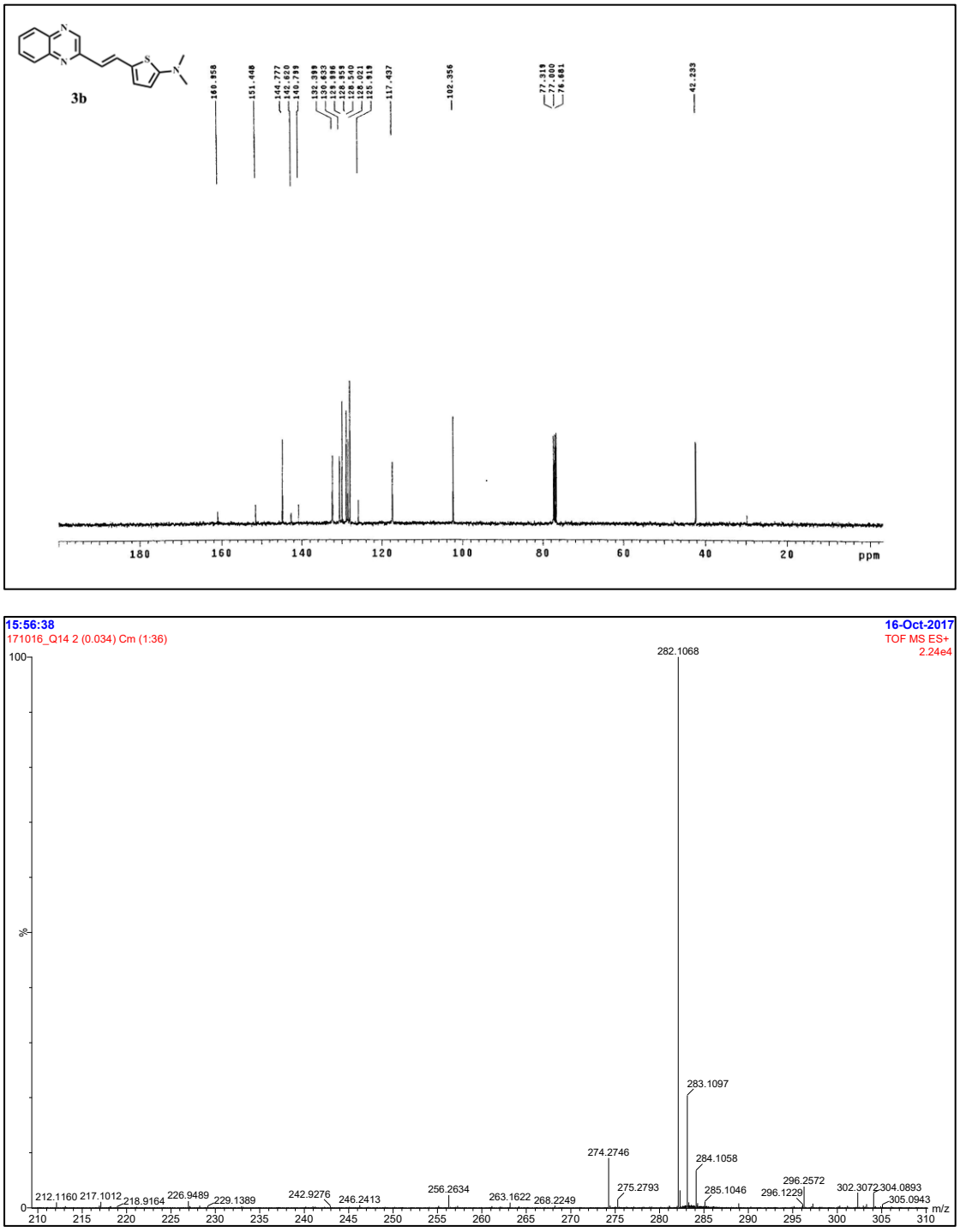

Fig. S6 ^{1}H-NMR, ^{13}C-NMR and HRMS data of **3b**.

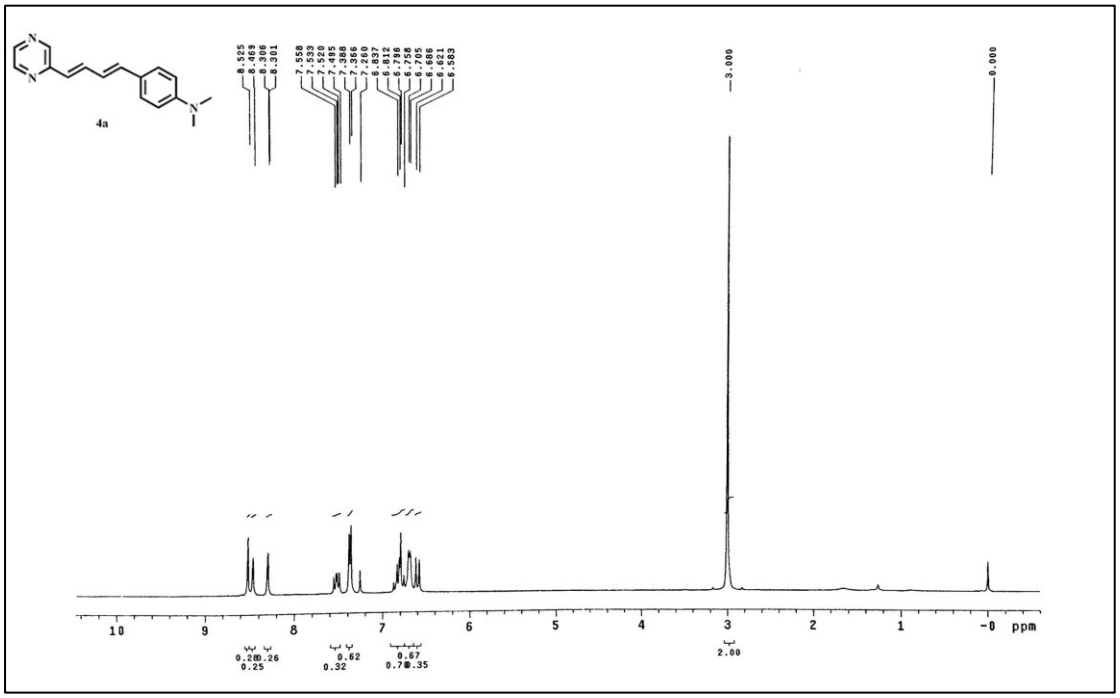
4a
8.525
8.465
8.306
8.301
7.558
7.539
7.530
7.495
7.388
7.366
7.356
6.857
6.812
6.796
6.758
6.705
6.686
6.621
6.583
3.000
0.000
10
9
8
7
6
5
4
3
2
1
-0
ppm
0.28
0.26
0.25
0.62
0.32
0.67
0.70
0.35
2.00

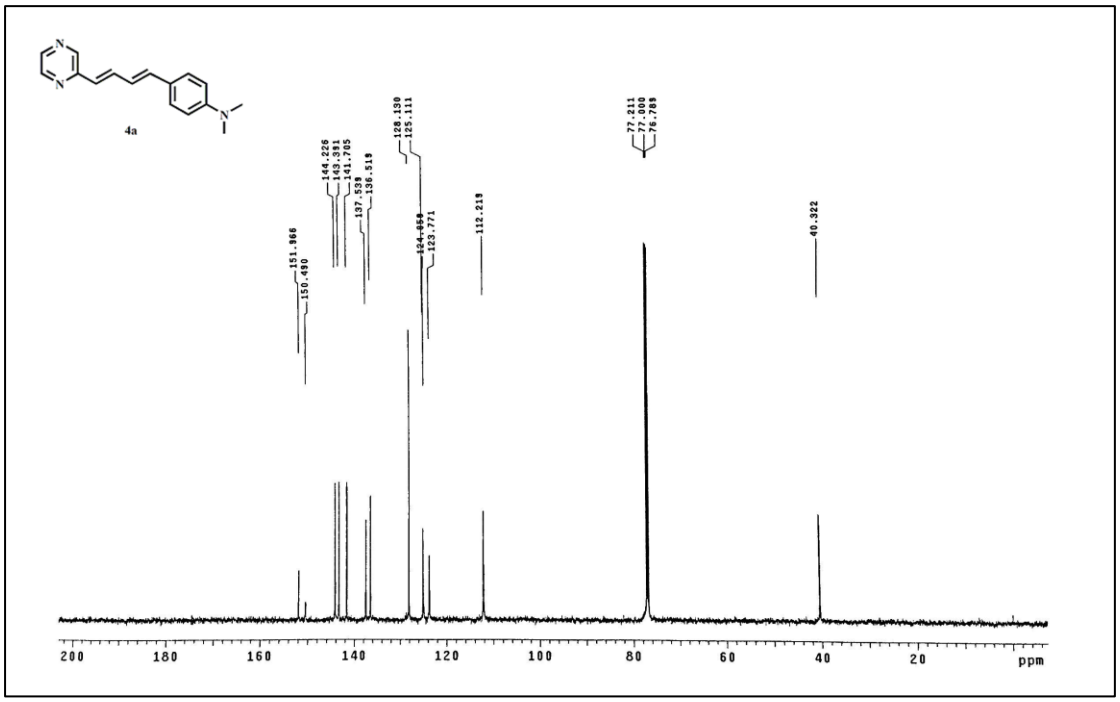
4a
151.866
150.480
144.225
143.881
141.705
137.539
136.519
128.130
125.111
124.059
123.771
112.219
77.211
77.000
76.788
40.322
200
180
160
140
120
100
80
60
40
20
ppm

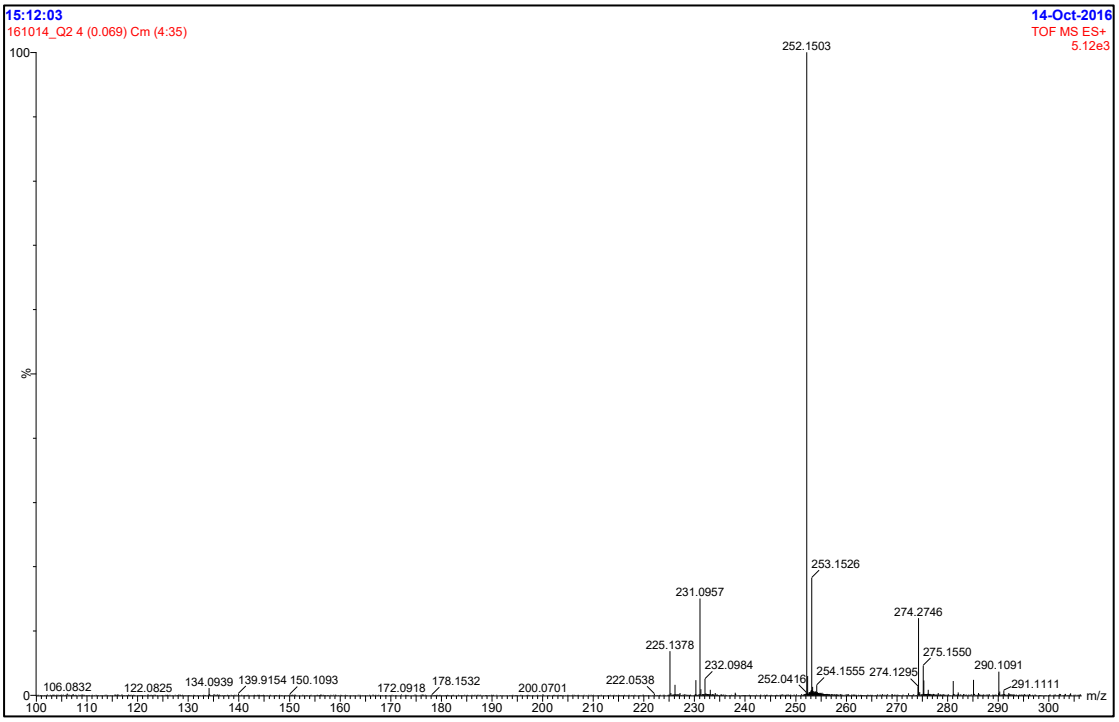

Fig. S7 ^{1}H-NMR, ^{13}C-NMR and HRMS data of **4a**.

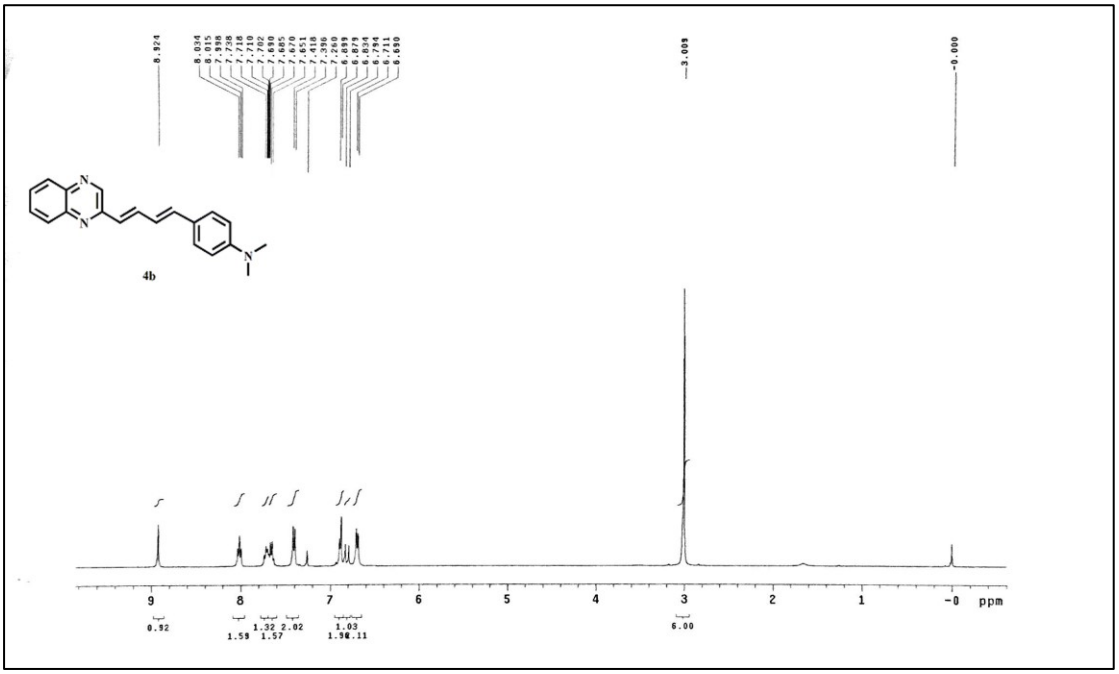

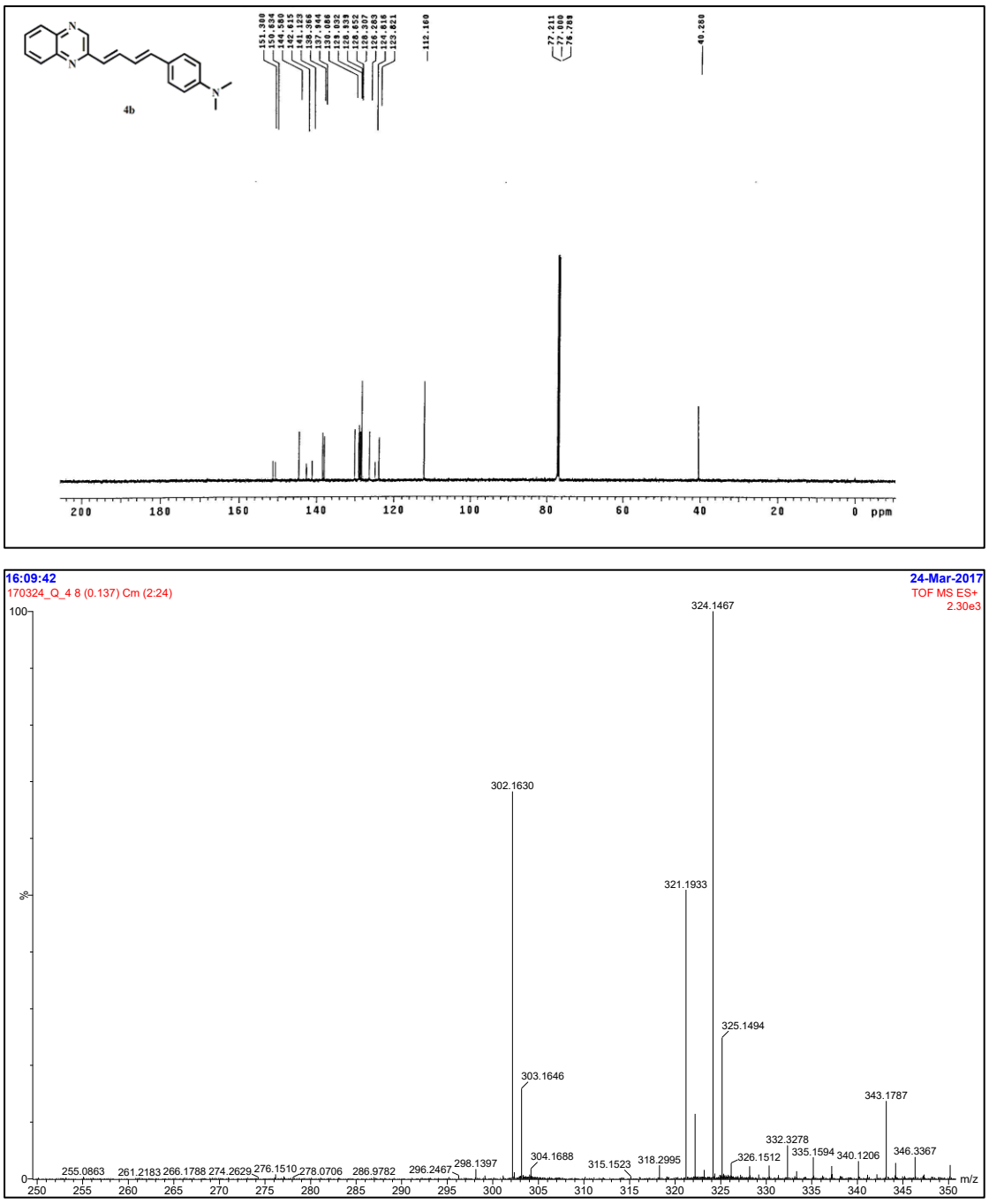

Fig. S8 ^{1}H-NMR, ^{13}C-NMR and HRMS data of **4b**.

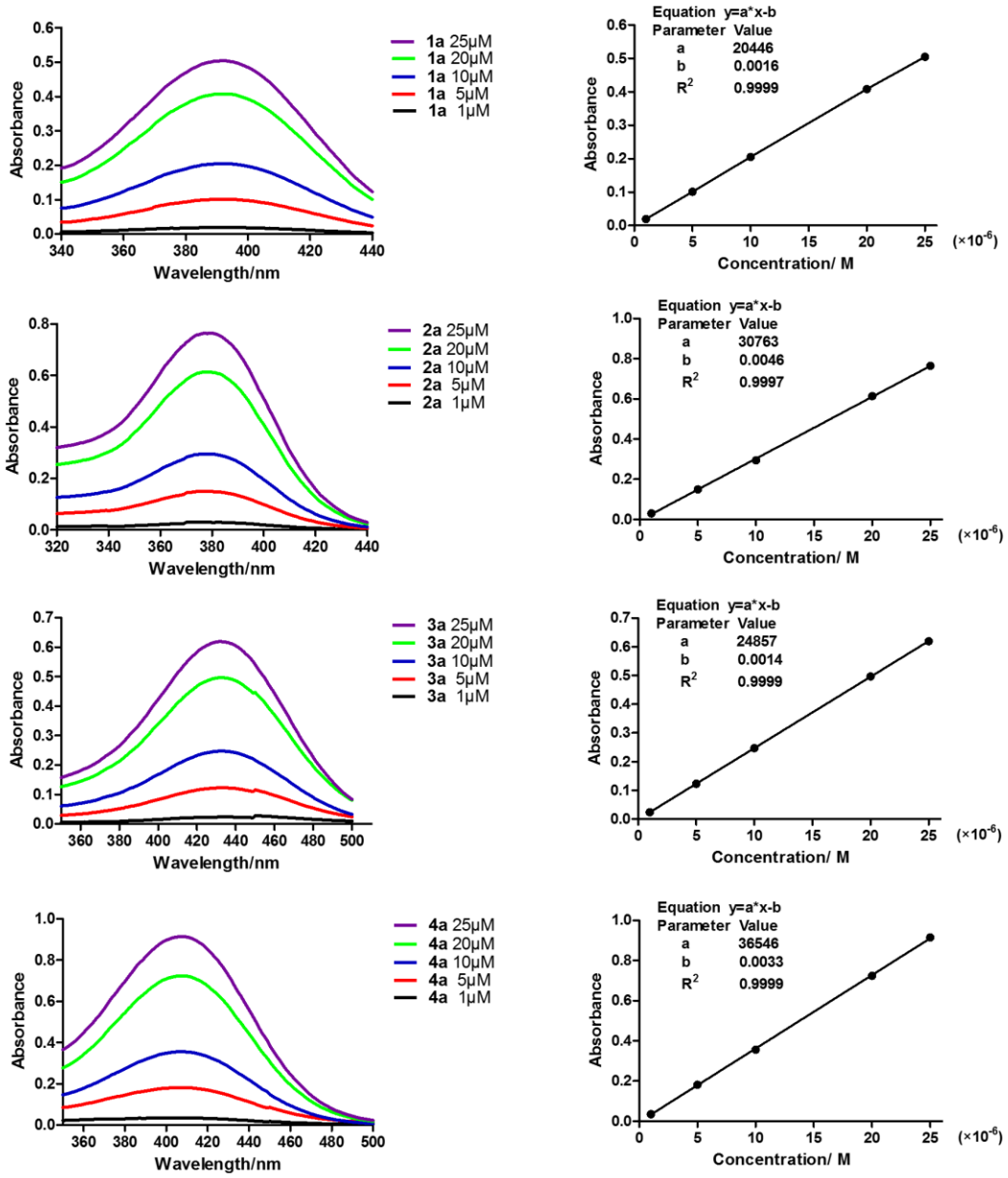

Fig. S9 Absorption spectra and molar absorption coefficient of **1-4 a** in ethanol.

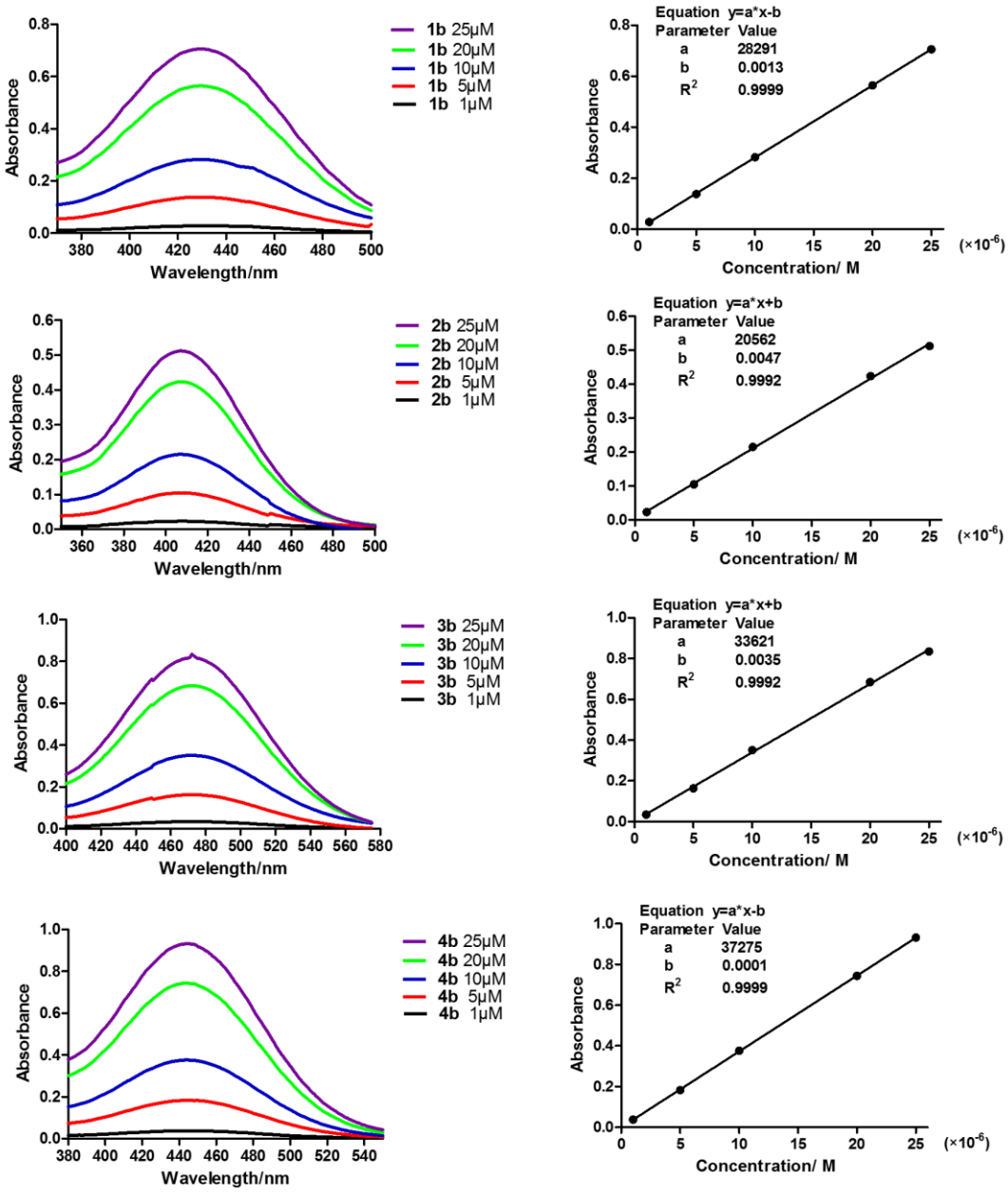

Fig. S10 Absorption spectra and molar absorption coefficient of **1-4 b** in ethanol.

Table S1. Fluorescence Profile

compd	λ_{abs} (nm)[a]	λ_{ex} (nm)[a]	λ_{em} (nm)[a]	ε ($M^{-1}cm^{-1}$)[a]	Φ (%)[a, b]
1a	392	404	536	20446	8.2
1b	426	442	570	28291	1.7
2a	380	396	532	30763	37.6
2b	408	426	568	20562	21.8
3a	433	451	553	24857	2.4
3b	472	482	603	33621	1.1
4a	408	420	558	36546	4.3
4b	442	464	583	37275	2.9

[a]Maximum absorbance wavelength (λ_{abs}), molar absorption coefficient (ε), maximum excitation wavelength (λ_{ex}), maximum emission wavelength (λ_{em}), and fluorescence quantum yield (Φ) were tested in ethanol. [b]Rhodamine B was taken as a reference fluorophore for measuring fluorescence quantum yield.

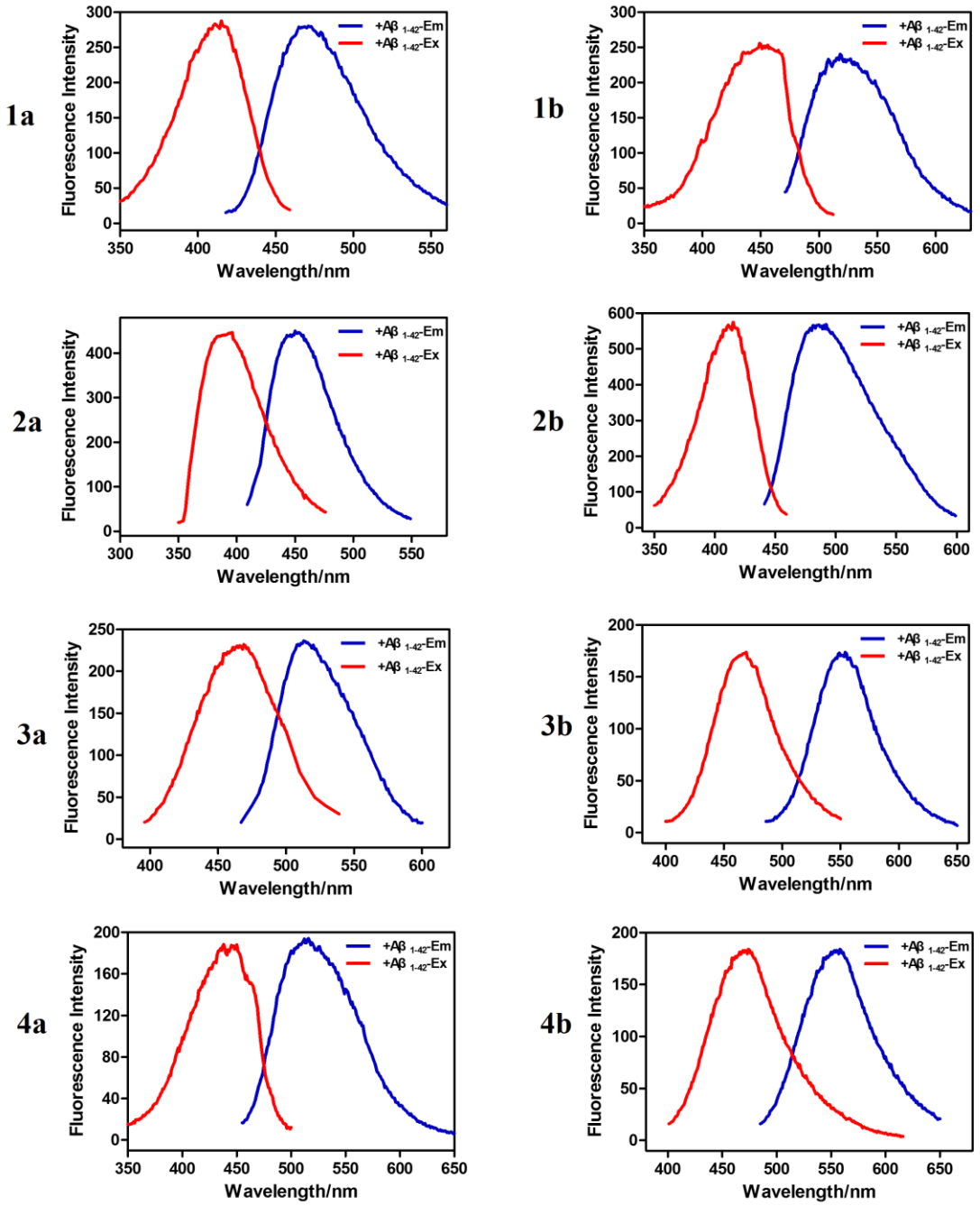

Fig. S11 Fluorescence excitation (Ex) and emission (Em) spectra of QNNs (1 μM) with $A\beta_{1\text{-}42}$ aggregates (2.75 μM).

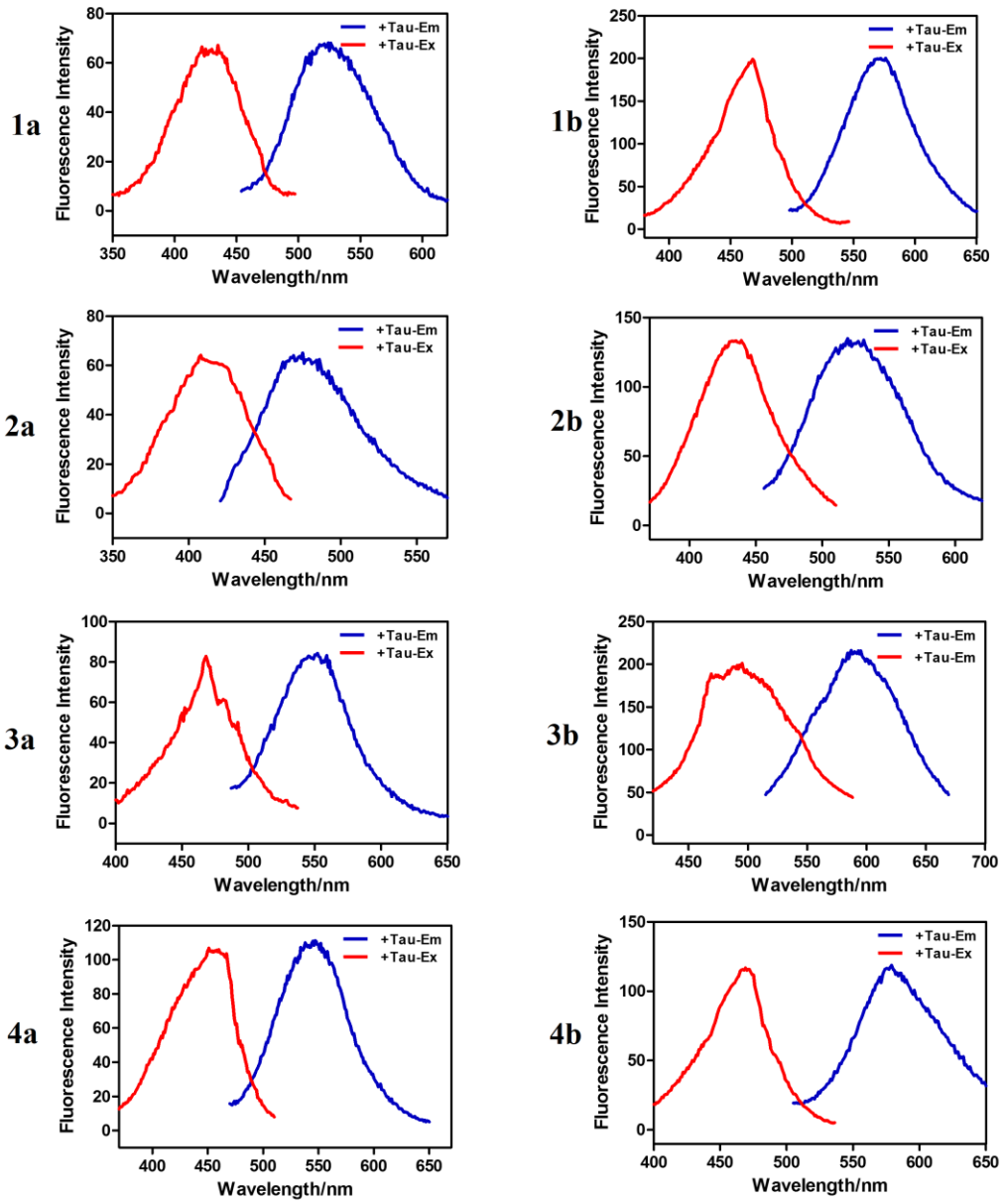

Fig. S12 Fluorescence excitation (Ex) and emission (Em) spectra of QNNs (1 μM) with tau aggregates (2.75 μM).

Table S2. Binding behavior of QNNs to tau aggregates and Aβ aggregates

compd	Fold increase[a]		Φ (%)[b]		Blueshift (nm)[c]		K_d (nM)[d]	
	tau	Aβ	tau	Aβ	tau	Aβ	tau	Aβ
1a	24	100	7.1	60.8	*n.s.*	62	121.1 ± 13.1	162.6 ± 6.8
1b	62	75	42.0	61.2	*n.s.*	65	35.2 ± 1.9	86.2 ± 5.8
2a	28	201	7.4	97.9	51	78	166.4 ± 10.3	76.3 ± 6.4
2b	64	292	34.5	100.4	41	81	51.9 ± 3.5	55.1 ± 7.8
3a	33	94	12.0	68.9	*n.s.*	41	114.3 ± 6.2	233.1 ± 27.9
3b	97	78	52.2	49.4	*n.s.*	48	25.2 ± 3.3	127.4 ± 13.3
4a	69	77	25.5	30.5	*n.s.*	43	53.1 ± 0.9	117.4 ± 0.9
4b	70	103	25.7	45.1	*n.s*	22	44.7 ± 3.6	77.9 ± 1.2

[a]Fold increase was determined by the ratio of fluorescence intensity (FI) of the probe in PBS solution with/without tau aggregates or $A\beta_{1\text{-}42}$ aggregates (2.75 μM). [b]Fluorescence quantum yields and [c]blueshift in emission of the probes upon binding. [d]Dissociation constant (K_d) was determined with results given as the mean ± SD (n = 3).

n.s. represents not significant.

Binding Specificity. To further determine the binding specificity of **3b**, fluorescence spectral change upon mixing with soluble tau or $A\beta_{1\text{-}42}$ species, were also tested. Incubation of **3b** with monomeric or oligomeric tau/$A\beta_{1\text{-}42}$ species showed weak change in fluorescence. Furthermore, **3b** showed moderate change upon mixing with α-synuclein aggregates, which is the assembly form of prion protein α-synuclein that shares common cross β-sheet structure with tau or Aβ aggregates.[3] These results further indicate good specificity of **3b** to tau aggregates.

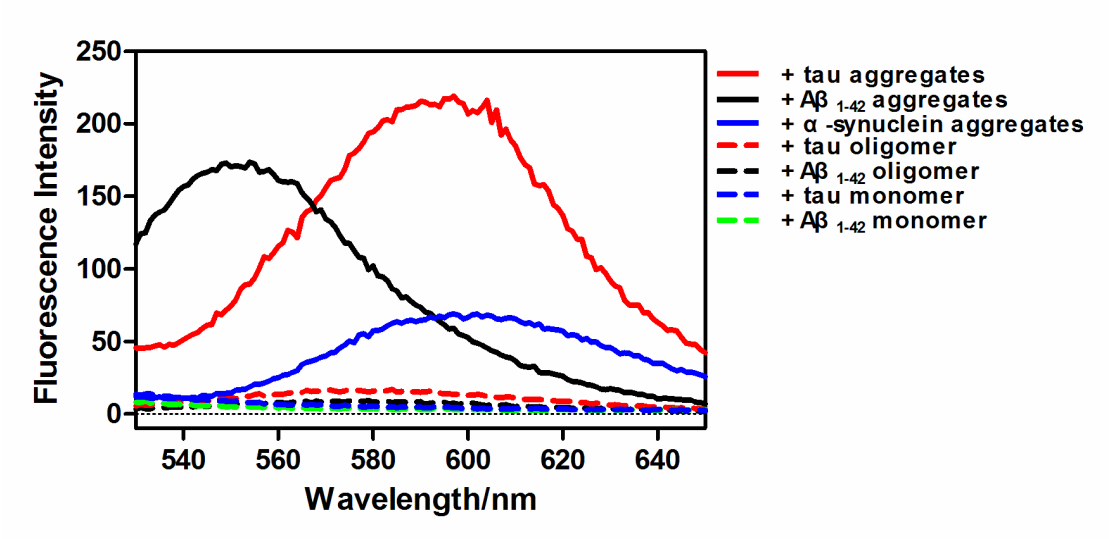

Fig. S13 Fluorescence emission spectra of **3b** (1 μM) with 2.75 μM of tau aggregates, $A\beta_{1\text{-}42}$ aggregates, α-synuclein aggregates, tau oligomer, Aβ oligomer, tau monomer and Aβ monomer.

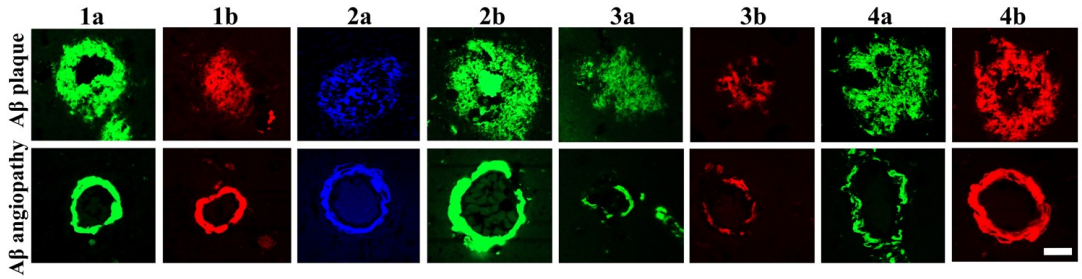

Fig. S14 Fluorescence staining of Aβ pathology of brain sections from an AD patient (6-μm-thick, temporal lobe, male, 85 years old) by QNNs: **3b** showed relatively weak fluorescence upon binding to Aβ plaques and Aβ angiopathy. Scale bar: 20 μm.

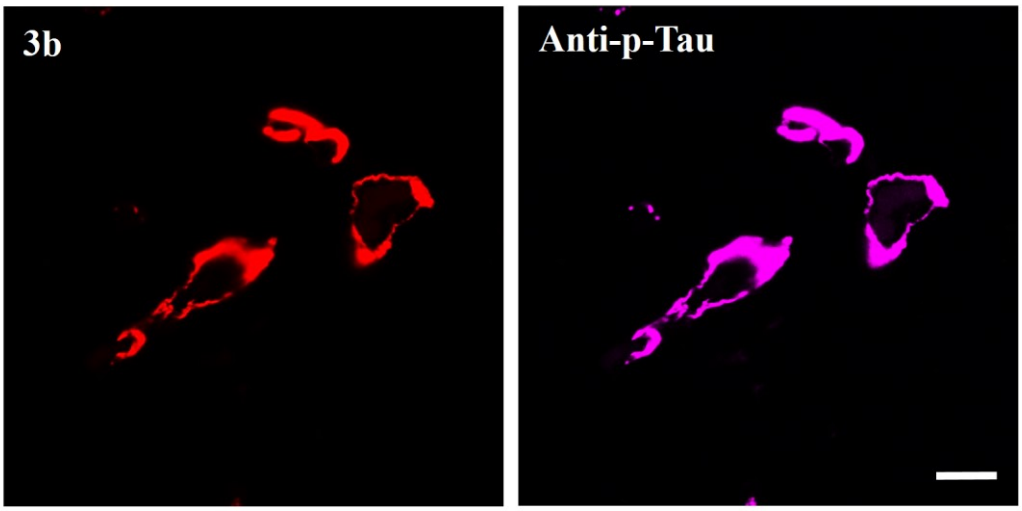

Fig. S15 Fluorescence staining of **3b** in brain sections from an AD patient (6-μm-thick, temporal lobe, male, 85 years old). **3b** (left) showed good colocalization with immunostained tau tangles (right). Scale bar: 20 μm.

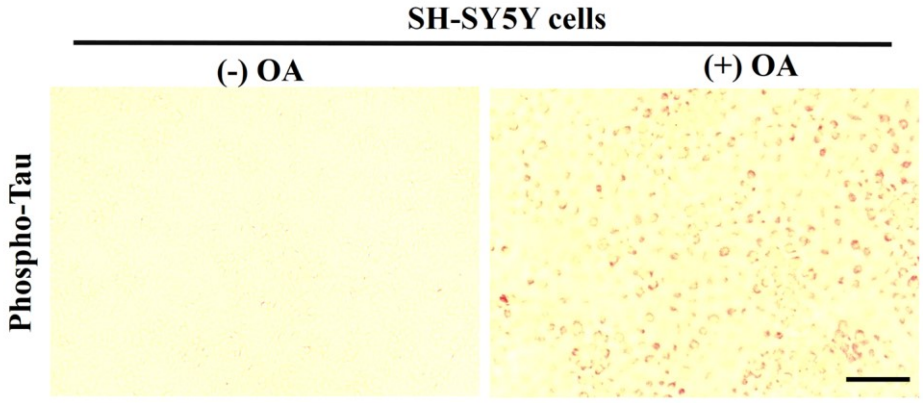

Fig. S16 Immunocytochemistry of SH-SY5Y cells before and after 3 h treatment with 100 nM of okadaic acid (OA). The OA-treated group showed substantial staining of chromogen, indicating the formation of intracellular tau aggregates. Scale bar: 200 μm.

Table S3. Brain uptake (%ID/g) of QNNs at 2, 10, 30, and 60 min postinjection in normal mice.

			Time after injection (min)				
Compd	Mw[a]	cLog *P*[a]	2	10	30	60	$Brain_{2min}/Brain_{60min}$
1a	225	2.26	15.42 ± 2.86	2.11 ± 0.45	0.45 ± 0.05	0.16 ± 0.07	98.35
1b	275	4.10	6.74 ± 0.77	4.17 ± 0.25	1.92 ± 0.33	0.51 ± 0.01	13.32
2a	226	1.64	12.61 ± 0.79	1.62 ± 0.40	0.25 ± 0.01	0.11 ± 0.01	112.43
2b	276	3.48	10.88 ± 0.44	3.91 ± 0.31	0.81 ± 0.06	0.43 ± 0.02	25.25
3a	231	2.43	13.12 ± 1.55	2.00 ± 0.40	0.41 ± 0.02	0.18 ± 0.08	72.91
3b	281	4.27	6.39 ± 0.65	3.78 ± 0.40	2.20 ± 0.52	0.52 ± 0.09	12.32
4a	251	2.77	13.29 ± 2.96	6.65 ± 0.38	1.75 ± 0.20	0.44 ± 0.15	33.87
4b	301	4.62	5.31 ± 0.29	3.71 ± 0.04	2.76 ± 0.16	0.64 ± 0.20	8.27

[a]Molecular weight (Mw) and clog *P* were calculated using ChemDraw Ultra 12.0.

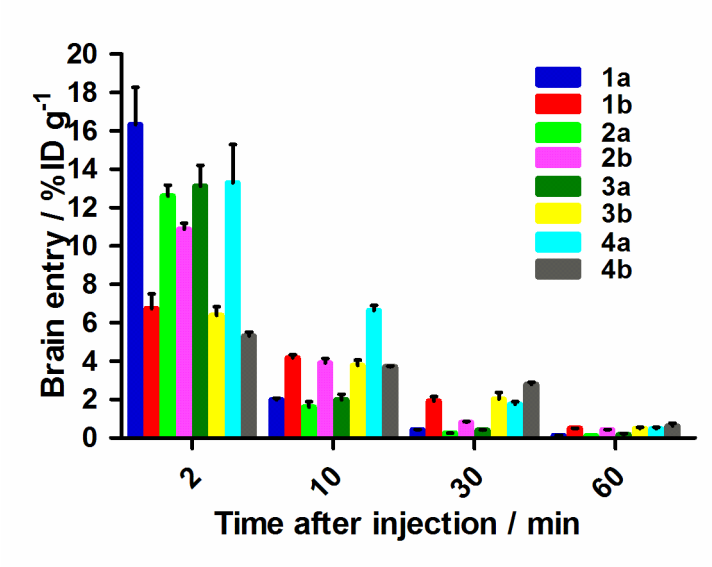

Fig. S17 Brain uptake of QNNs in normal mice at different timepoints (n = 3 per timepoint). Quantitative data were determined by HPLC and expressed as percent injected dose per gram of tissue (%ID/g).

Table S4. Blood clearance and brain/blood ratio of **3b** at 2, 10, 30, and 60 min postinjection in normal mice.

	Time after injection (min)			
	2	10	30	60
Blood uptake (%ID/g)	2.18 ± 0.08	1.38 ± 0.09	0.33 ± 0.04	0.14 ± 0.003
brain/blood ratio	2.93	2.74	6.67	3.71

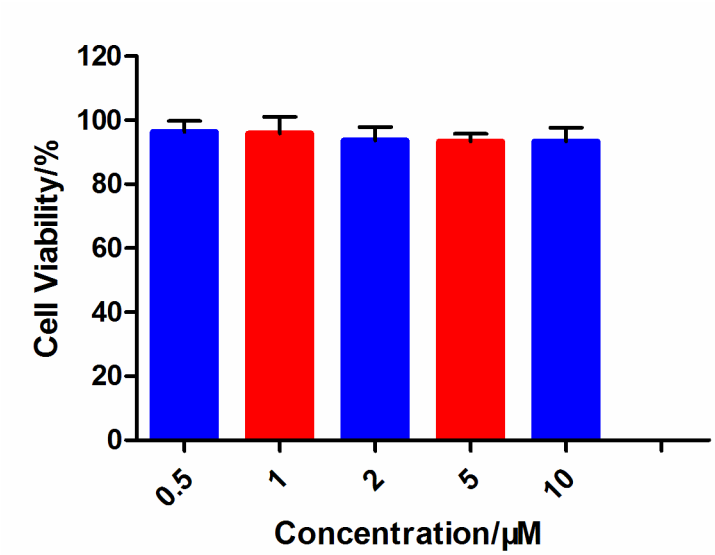

Fig. S18 Cell viability after incubation of **3b** at different concentrations with SH-SY5Y cells by MTT assay. No significant toxicity was found at 10 μM.

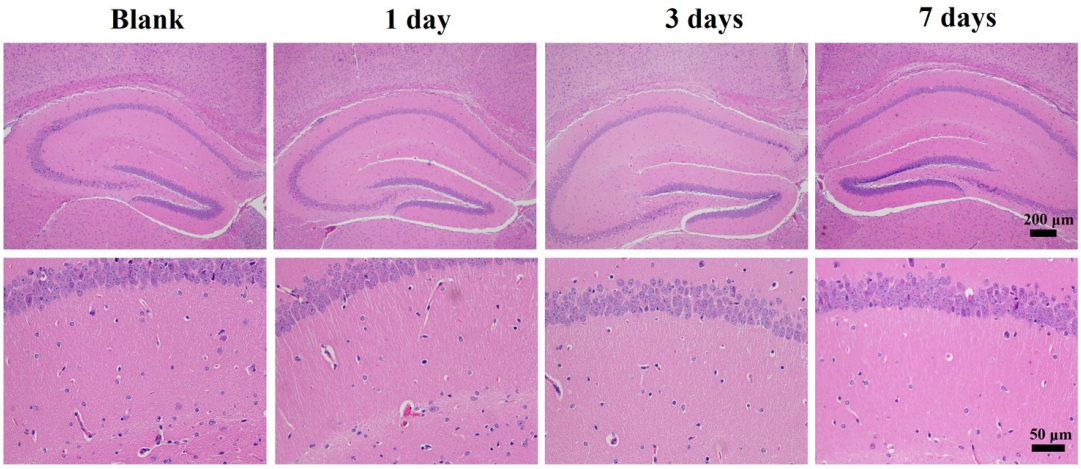

Fig. S19 Representative histopathological images of brain sections of normal mice (n = 3) with hematoxylin and eosin (H&E) staining at different days after intravenous injection of **3b** (3.0 mg/kg, 45% DMSO and 55% propylene glycol)**.** No typical lesions, inflammation or focal necrosis were observed, indicating no significant toxicity of the probe to the brain.

In Vivo Imaging. In vivo imaging of normal nude mice was first conducted, and real-time images showed that **3b** efficiently crossed BBB with strong fluorescence in the brain region as early as 5 min and fluorescence signals diminished with time over 60 min, suggesting low nonspecific signals from unbound probe (Fig. S20). To assess the potential of **3b** for specific imaging of cerebral tau aggregates, in vivo near infrared fluorescence imaging was performed using P301S tau transgenic mice, which are a line of transgenic mice that develop filamentous tau inclusions in the brain from 6 months of age, and progressively accumulate tau tangles with neuronal loss at 9-12 months.[7] P301S tau transgenic mice (9 months) were selected in the present study, and age-matched C57BL/6 mice were selected as wild-type controls, and APP/PS1 transgenic mice (9 months), with marked cerebral Aβ plaques, were also used under the same imaging condition for comparison. As shown in Fig. S21, after intravenous injection of **3b**, fluorescence signals from brain area diminished more slowly in the P301S tau group than in the wild-type control and APP/PS1 group. Semi-quantitative analysis of region of interest (ROI) in the brains showed significant difference in fluorescence clearance profiles among these three groups: fluorescence washout was significantly slower in brain regions of the P301S tau group than those of the wild-type control and APP/PS1 group. Ex vivo fluorescent observation of the brains APP/PS1 brains after in vivo imaging further confirmed moderate fluorescence signals from Aβ binding under the same imaging condition (Fig. S22).

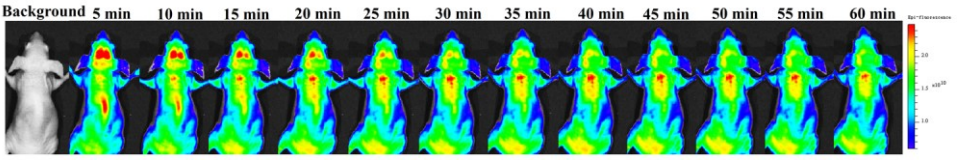

Fig. S20 Real-time fluorescence imaging (excitation = 500 nm; emission = 620 nm) in a normal nude mouse after intravenous injection of **3b** (3.0 mg/kg, 45% DMSO and 55% propylene glycol).

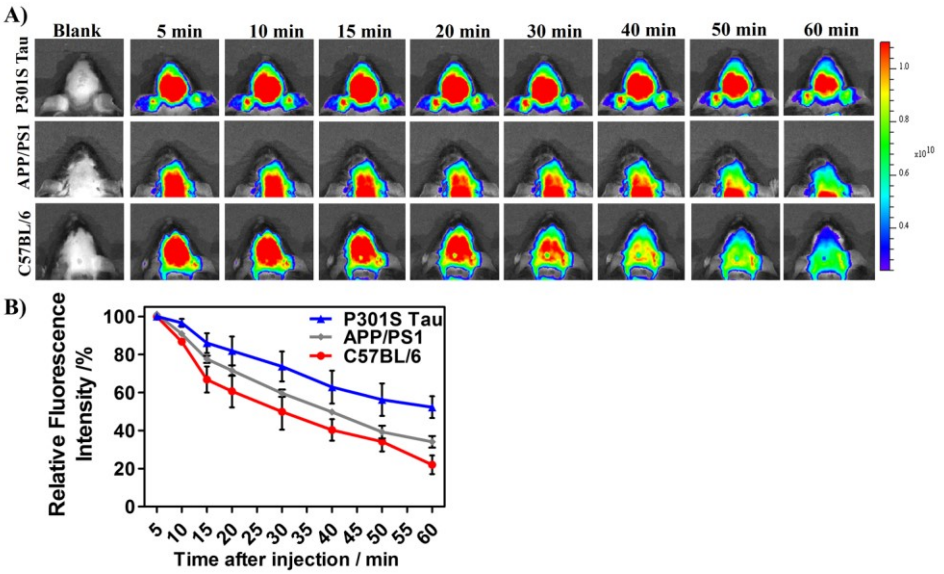

Fig. S21 Real-time fluorescence imaging and relative fluorescence intensity in the brains of P301S tau transgenic mice, APP/PS1 mice and C57BL/6 mice after intravenous injection of **3b** (3.0 mg/kg, 45% DMSO and 55% propylene glycol).

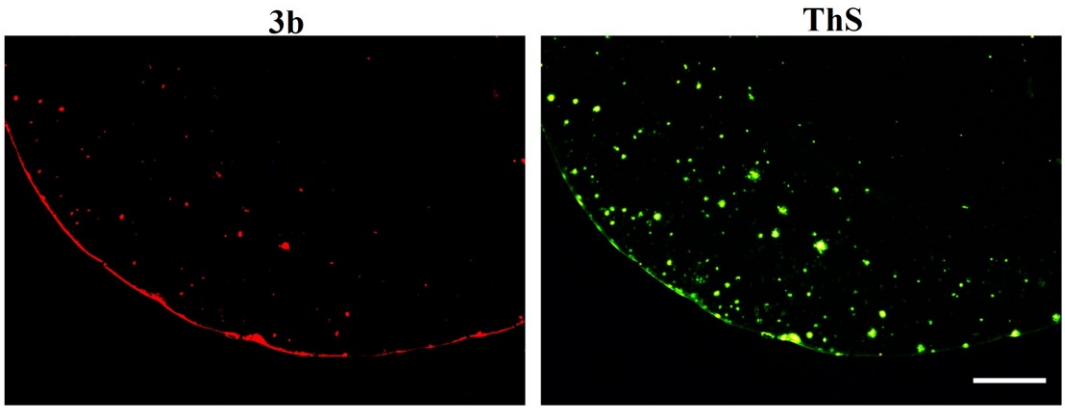

Fig. S22 Ex vivo fluorescence observation of brain sections from APP/PS1 mice after intravenous injection of **3b**. The presence of Aβ plaques was confirmed by subsequent staining with ThS. Scale bar: 400 μm.

References

1 M. von Bergen, S. Barghorn, L. Li, A. Marx, J. Biernat, E. M. Mandelkow and E. Mandelkow, *J. Biol. Chem.*, 2001, **276**, 48165.

2 B. Y. Zhu, Y. Cheng, G. B. Li, S. Y. Yang and Z. R. Zhang, *Bioorg. Med. Chem.*, 2016, **24**, 827.

3 (a) J. Ries, V. Udayar, A. Soragni, S. Hornemann, K. P. Nilsson, R. Riek, C. Hock, H. Ewers, A. A. Aguzzi and L. Rajendran, *ACS Chem. Neurosci.*, 2013, **4**, 1057. (b) M. T. Fodero-Tavoletti, R. S. Mulligan, N. Okamura, S. Furumoto, C. C. Rowe, Y. Kudo, C. L. Masters, R. Cappai, K. Yanai and V. L. Villemagne, *Eur. J. Pharmacol.*, 2009, **617**, 54.

4 (a) X. Zhang, Y. Tian, Z. Li, X. Tian, H. Sun, H. Liu, A. Moore and C. Ran, *J. Am. Chem. Soc.*, 2013, **135**, 16397. (b) S. Taniguchi, N. Suzuki, M. Masuda, S. Hisanaga, T. Iwatsubo, M. Goedert and M. Hasegawa, *J. Biol. Chem.*, 2005, **280**,

7614.

5 D. Su, J. Oh, S. Lee, J. M. Lim, S. Sahu, X. Yu, D. Kim and Y. Chang. *Chem. Sci*., 2014, **5**, 4812.

6 H. Fu, M. Cui, L. Zhao, P. Tu, K. Zhou, J. Dai and B. Liu, *J. Med. Chem.*, 2015, **58**, 6972.

7 Y. Yoshiyama, M. Higuchi, B. Zhang, S. M. Huang, N. Iwata, T. C. Saido, J. Maeda, T. Suhara, J. Q. Trojanowski, and V. M. Lee V. *Neuron*., 2007, **53**, 337.